

## Advances in Supported Amine Adsorbents for Direct Air Capture of CO<sub>2</sub>

Maryna Shakoor<sup>1</sup>, Danianla Battezzore<sup>2,\*</sup>

<sup>1</sup> Center for Advanced Materials (CAM), Qatar University, 2713 Doha, Qatar

<sup>2</sup> Dipartimento di Scienza Applicata e Tecnologia, Politecnico di Torino, Alessandria site, Viale Teresa Michel 5, 15121 Alessandria, Italy

\*Corresponding author: DBattezzore@polito.it

**Abstract.** Amid escalating global climate change, carbon dioxide (CO<sub>2</sub>) direct air capture (DAC) technology has emerged as a critical solution for mitigating greenhouse gas emissions. Central to this technology are supported amine adsorbents, which have attracted considerable attention due to their unique properties and potential applications. However, these materials still face significant challenges, including limited adsorption capacity, insufficient selectivity, high costs, and inadequate long-term stability. This article provided a comprehensive review of recent advancements in supported amine adsorbents, focusing on three primary synthesis methods: impregnation, grafting, and in-situ polymerization. Impregnation, known for its simplicity and cost-effectiveness, is suitable for large-scale production but suffers from poor stability of the loaded amines. Grafting enhances amine stability through chemical bonding, yet its complex synthesis process and high costs hinder widespread adoption. In-situ polymerization, which enables uniform amine distribution via polymerization techniques, exhibits superior adsorption performance but remains technically challenging for industrial-scale applications. Furthermore, this review delved into the critical factors influencing adsorption performance, such as temperature, humidity, and carrier material properties, emphasizing that optimizing these parameters can significantly enhance adsorbent efficiency. Notably, in-situ polymerization adsorbents demonstrated exceptional potential for structural control, offering opportunities to improve both adsorption capacity and kinetics. Despite the promising prospects of supported amine DAC adsorbents, several challenges must be addressed to advance their practical application. This article proposed that future research should prioritize performance optimization and cost reduction, aiming to develop highly efficient, stable, and economically viable adsorbents. Additionally, interdisciplinary efforts are essential to explore novel carrier materials and innovative synthesis strategies, thereby providing robust theoretical and technical foundations for industrial deployment. Through sustained innovation and technological breakthroughs, supported amine DAC adsorbents are poised to play a pivotal role in achieving global sustainability goals and offering viable solutions to combat climate change.

**Keywords:** Carbon dioxide; Direct air capture; Amine-functionalized; Solid adsorbent; Solid amines

Received on 15 Feb 2025, Accepted on 15 April 2025, Published on 15 May 2025

Copyright © 2025 Maryna Shakoor and Danianla Battezzore *et al.* licensed to JGEEE. This is an open access article distributed under the terms of the CC BY-NC-SA 4.0, which permits copying, redistributing, remixing, transformation, and building upon the material in any medium so long as the original work is properly cited.

### 1 Introduction

Achieving carbon peaking and promoting carbon neutrality have become global focal points, and carbon capture methods are a necessary pathway to reach these dual carbon goals. However, contemporary carbon capture efforts predominantly focus on CO<sub>2</sub> separation from post-combustion flue gases emitted by large stationary point sources such as power generation facilities and petroleum refineries. While effective large-scale capture for nearly 50% of total CO<sub>2</sub> emissions from mobile distributed sources has not yet been established, necessitating urgent development of related technologies. Direct Air Capture (DAC) denotes the technological approach of extracting CO<sub>2</sub> directly from ambient atmospheric conditions for subsequent sequestration or valorization. The capture process is not limited by time or location, and features flexible deployment and low land/water resource occupancy. It can not only offset emissions from hard-to-decarbonize mobile sources but also combine with renewable energy to achieve net negative emissions. Direct Air Capture (DAC) denotes the technological approach of extracting CO<sub>2</sub> directly from ambient atmospheric conditions for subsequent

sequestration or valorization. The International Energy Agency's 2050 Net Zero Emissions Roadmap and China's Carbon Dioxide Capture, Utilization and Storage (CCUS) Pathway Research Report both indicate that DAC will constitute an essential technological element for achieving carbon neutrality both globally and within China. It is estimated that by 2050, its capture volume will account for over 13% of all carbon capture.

Currently, DAC technology primarily employs solution absorption and solid adsorption methods. The solution absorption method mainly uses alkali or alkaline earth metal hydroxides to capture CO<sub>2</sub> through causticization or alternative causticization processes, requiring reliance on high-temperature heat sources of 800-1000°C for regeneration, and faces risks like corrosion and solution volatilization. These issues limit its development and application. The adsorption method uses solid adsorbents to capture CO<sub>2</sub> from the air, requiring a lower regeneration temperature (80-200°C), holds promise for lower capture energy consumption, and adsorption columns allow for flexible structural optimization. Using industrial waste to synthesize adsorbents can enhance the sustainability of the adsorption process, making it a current focus of DAC research. Various types of solid materials are applied in solid adsorption DAC, and based on the binding principles between the adsorbent and CO<sub>2</sub>, they can be classified into physical adsorbents and chemical adsorbents. Among them, physical adsorbents capture CO<sub>2</sub> through intermolecular forces, with fast adsorption/desorption kinetics, and the weaker binding force makes CO<sub>2</sub> easy to desorb. However, at extremely low CO<sub>2</sub> concentrations, physical adsorbents have low selectivity and small adsorption capacity for CO<sub>2</sub>, and are easily affected by competitive adsorption of water. Currently, their application in DAC still faces significant challenges.

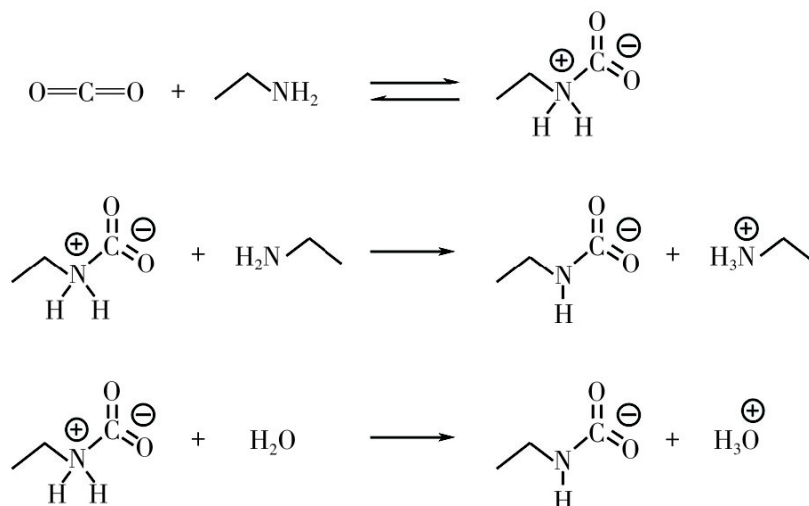


**Figure 1** Reaction mechanism of solid amine in capturing CO<sub>2</sub> process [17]

Chemical adsorbents employ reactive processes between the material and CO<sub>2</sub> to accomplish capture. Chemical adsorbents employ reactive processes between the material and CO<sub>2</sub> to accomplish capture, exhibiting elevated selectivity and substantial uptake capacity even at extremely dilute CO<sub>2</sub> concentrations. Among these, amine-functionalized porous materials (namely, supported amines) currently represent one of the most extensively deployed chemical adsorbent classes for DAC applications. They are prepared by loading organic amines onto porous solids in specific ways. The porous solid, with its developed pore structure, acts as a carrier for accommodating and dispersing the organic amines, while the amino groups in the organic amines can selectively react with CO<sub>2</sub>. Under anhydrous conditions, the predominant reaction mechanism proceeds as follows: the primary amine moiety undergoes reaction with CO<sub>2</sub> to generate a zwitterionic intermediate, which subsequently undergoes deprotonation through interaction with a secondary amine functionality, yielding carbamate salt or ester products. Consequently, the stoichiometric requirement for sequestering 1 mol of CO<sub>2</sub> necessitates 2 mol of amine functional groups. Consequently, the stoichiometric requirement for sequestering 1 mol of CO<sub>2</sub> necessitates 2 mol of amine functional groups, establishing a theoretical maximum amine efficiency (defined as the molar ratio of captured CO<sub>2</sub> to N element in the material) of 0.5. Under humid conditions, water molecules or hydroxide ions may functionally replace the secondary amine group to facilitate deprotonation. Under humid conditions, water molecules or hydroxide ions may functionally replace the secondary amine group to facilitate

deprotonation, enabling theoretical amine efficiency to approach unity. Furthermore, Under humid conditions, water molecules or hydroxide ions may functionally replace the secondary amine group to facilitate deprotonation, enabling theoretical amine efficiency to approach unity. Furthermore, an alternative reaction pathway generating ammonium bicarbonate may additionally proceed under moisture-present conditions, Under humid conditions, water molecules or hydroxide ions may functionally replace the secondary amine group to facilitate deprotonation, enabling theoretical amine efficiency to approach unity. Furthermore, an alternative reaction pathway generating ammonium bicarbonate may additionally proceed under moisture-present conditions, likewise achieving theoretical amine efficiency of 1. Consequently, in contrast to physical adsorbents, supported amine materials enable selective CO<sub>2</sub> capture across both anhydrous and moisture-containing environments.

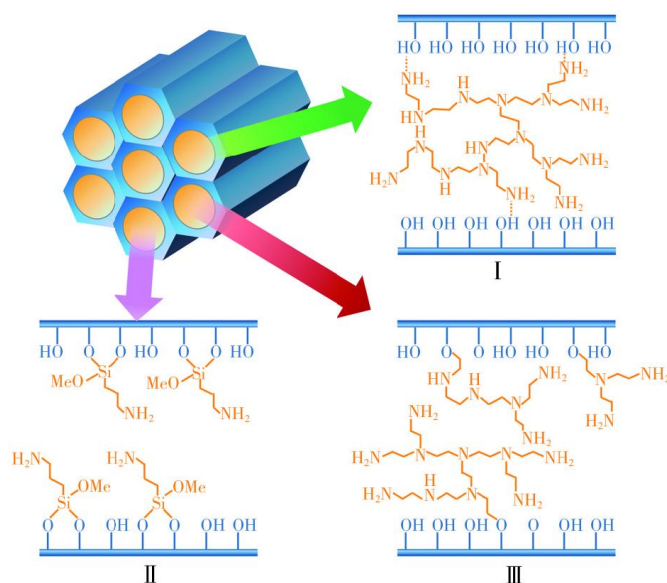


**Figure 2** Three types of solid amines[18]

Facilitating practical deployment within authentic atmospheric conditions. Nevertheless, enhancing DAC performance while minimizing its energy demands and operational expenses necessitates that adsorbents satisfy real-world criteria regarding uptake capacity, reaction rates, regeneration energy requirements, and structural durability. The efficacy of immobilized amines is intimately connected to their fabrication approach and precursor characteristics, along with experimental parameters, demanding thorough comprehension grounded in mechanistic insights, integrated with physicochemical property evaluation and systematic benchmarking for their deployment in DAC contexts. Based on the bonding principle between the organic amine and the support, supported amines are mainly divided into three types, as shown in Fig. 2. Impregnated supported amines (Class I) are prepared by physically mixing organic amines with porous supports, where the amines are connected to the support via intermolecular forces like hydrogen bonds, featuring easy synthesis. Typically, amines with large molecular weight are used to prevent excessive amine volatilization, and the impregnation method allows for higher amine loading, giving the material high adsorption capacity. Grafted supported amines (Class II) are prepared via covalent grafting, based on the principle of small-molecule amines reacting with porous supports under specific conditions, fixing amine groups onto the support surface through covalent bonds (such as C-O, C-N, or Si-O bonds). Due to the strong force of covalent bonds, these materials are less prone to amine leaching during use, exhibiting excellent stability. Nevertheless, covalent attachment is typically constrained by the quantity of reactive sites available on the substrate surface, leading to diminished amine content and consequently modest uptake capacity of the resulting material. Despite this, their high stability and controllability make them important for applications like CO<sub>2</sub> capture. In-situ polymerized supported amines (Class III) are prepared by conducting in-situ polymerization of amine monomers on and within porous supports. This type of material can also be considered a special type of grafted supported amine. Based on having amine-support covalent bonds, it also possesses high loading similar to impregnated supported amines, combining the advantages of both. However, its synthesis path generally has specific requirements for the types of support and

amine. This article will elaborate on the current research status of these three types of materials, compare their adsorption/desorption performance under different conditions, summarize the performance characteristics of different types of materials, and provide references for future development of efficient, tunable, and low-cost DAC adsorbents.

## 2 Impregnated Supported Amines

Impregnated amine-functionalized sorbents represent among the most prevalent CO<sub>2</sub> capture materials for direct air extraction, characterized by straightforward fabrication protocols, economical production, and adjustable performance attributes. along with extensive utilization across DAC applications. Impregnated amine-functionalized sorbents leverage the adsorptive properties and substantial surface area of porous substrates to distribute and infuse organic amines within the support's pore structure, yielding a CO<sub>2</sub> capture material. Different organic amines and porous supports have a decisive impact on the DAC performance of impregnated supported amines.

### 2.1 Effect of Amine Type

Different types of organic amines, due to differences in their molecular structure and the number of amine groups, exhibit significant differences in CO<sub>2</sub> adsorption capacity. Common organic amines for impregnated supported amines include polyethyleneimine (PEI) and tetraethylenepentamine (TEPA), etc.

Polyethyleneimine (PEI) can be divided into linear PEI and branched PEI based on its degree of polymerization. Linear PEI molecules have a more regular chain, which can present a more ordered loading state on certain specific porous supports, facilitating the diffusion of CO<sub>2</sub> molecules and adsorption reactions on its surface. Branched PEI has richer amino active sites compared to linear PEI. These amino active sites are key for chemical reactions with CO<sub>2</sub>. More amino groups mean the ability to bind with more CO<sub>2</sub> molecules. Therefore, under the same loading conditions, supported amines loaded with branched PEI will have higher adsorption capacity. Wei Wei et al. used the impregnation method to functionalize 13X molecular sieve with PEI as the amino functionalization material. The modified molecular sieve exhibited optimal CO<sub>2</sub> adsorption at 70°C. Shen Xuehua et al. used PEI as the organic amine, sodium aluminate and aluminum sulfate as raw materials, synthesized large pore volume Al<sub>2</sub>O<sub>3</sub> via azeotropic distillation, and synthesized an aluminum-based supported amine adsorbent, 60%PEI@Al<sub>2</sub>O<sub>3</sub>-4h, by impregnating PEI with the monolithic adsorbent at a 60% mass ratio. The CO<sub>2</sub> uptake capacity at saturation attained 4.5 mmol/g. This sorbent exhibited negligible degradation in capture performance following ten regeneration cycles. offering guidance for the development of economical, robust PEI-impregnated amine-functionalized sorbents. Illustrated in Figure 3 is the synthetic procedure for PEI-impregnated silica gel alongside the preparation of impregnated dry silica sol.

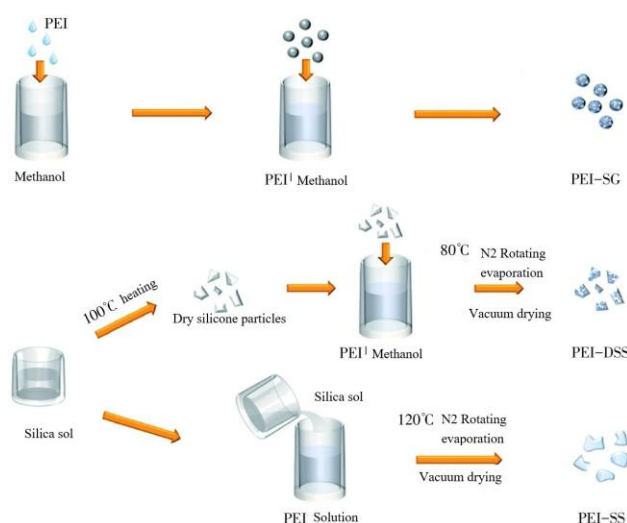


**Figure 3** Preparation process of polyethyleneimine-impregnated silica gel (PEI-SS) and

## polyethyleneimine-impregnated dried silica sol (PEI-DSS) [31]

Tetraethylenepentamine (TEPA) belongs to polyamine compounds, and its molecular structure contains multiple active amino hydrogen atoms. These hydrogen atoms give TEPA strong basicity and high reactivity towards CO<sub>2</sub>, enabling it to quickly react with CO<sub>2</sub> to form stable formates or bicarbonates. Gao Chenhui and colleagues synthesized TEPA-impregnated expanded vermiculite amine-functionalized sorbent (EV-TEPA) for carbon dioxide capture, examining the influence of TEPA content and thermal conditions on its uptake behavior. The findings revealed that expanded vermiculite subjected to elevated-temperature calcination exhibits substantial capacity for amine incorporation. EV-TEPA demonstrated optimal uptake performance at 75°C along with favorable regeneration stability. Wang Mingmei et al. combined TEPA with metal-organic framework material ZIF to prepare TEPA@Co/Zn-ZIF supported amine for adsorption and cycling experiments. Benefiting from the chemical reaction between TEPA and CO<sub>2</sub>, compared to ZIF-8 and Co/Zn-ZIF, the modified material's CO<sub>2</sub> adsorption capacity increased to 2.53 mmol/g. Shen Yao et al. encapsulated TEPA into MOF-808 pores to obtain TEPA@MOF-808. The adsorption capacity of this material increased by 2.15 times compared to MOF-808, with adsorption rate constant and selectivity increasing by 13% and 498%, respectively. After 10 cycles, the adsorption capacity decreased by 10.9%, indicating significantly improved performance and stability. This demonstrates that the TEPA-based amine modification approach can substantially improve CO<sub>2</sub> capture performance and durability.

The quantity of amine functionalities likewise constitutes a critical determinant governing the uptake capacity of impregnated amine-functionalized sorbents. Within a defined range, increasing organic amine content leads to enhanced CO<sub>2</sub> adsorption capacity, though excessive loading may cause pore blockage and reduced performance. The sorbent's uptake capacity exhibits an increasing pattern. This is because more organic amine means more adsorption active sites, capable of adsorbing more CO<sub>2</sub> molecules. However, when the loading exceeds a certain threshold, phenomena like agglomeration of organic amine on the support surface or pore blockage occur. The self-association of organic amines sequesters certain amino groups internally, denying them full availability for CO<sub>2</sub> interaction, while pore occlusion inhibits CO<sub>2</sub> molecular transport to interior active zones. Each scenario undermines overall adsorption effectiveness. As depicted in Figure 4, Miao and co-workers developed PEI/SBA-15 and TEPA/SBA-15 integrated sorbents with varied amine saturation levels. Gravimetric sorption tests conducted at 25°C in 400 ppm CO<sub>2</sub> environments demonstrated that CO<sub>2</sub> removal capacity does not increase linearly with impregnation ratio, and excessive amine introduction can produce deleterious consequences.

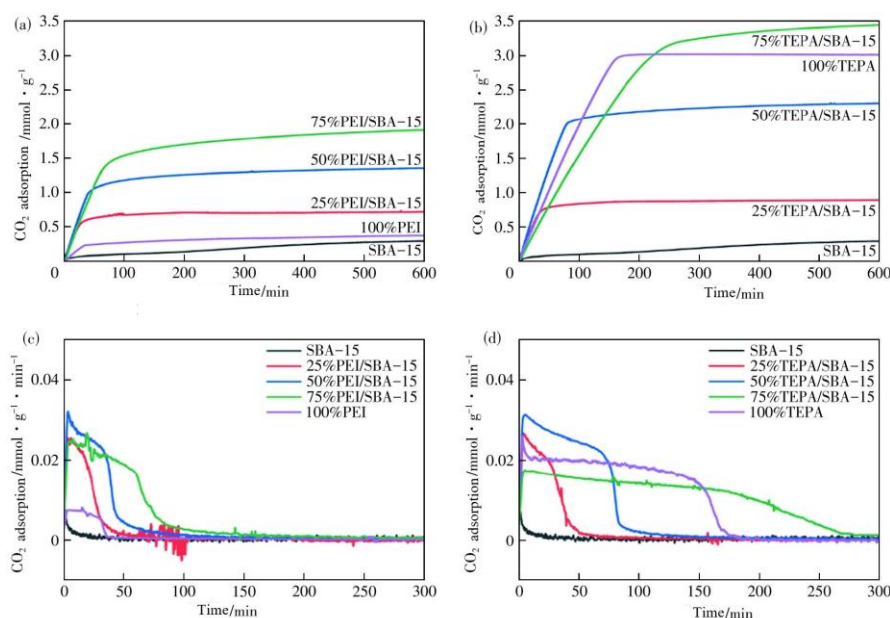


**Figure 4** Adsorption performance of PEI/SBA-15 and TEPA/SBA-15 composites with different amine impregnation amounts [37]

In terms of adsorption capacity, branched PEI, due to its rich and highly accessible amino group distribution, typically exhibits higher adsorption capacity compared to linear PEI. This gives supported amines prepared based on branched PEI a clear advantage when dealing with high-concentration CO<sub>2</sub> gas sources. However, although TEPA has numerous active amino hydrogen atoms in its molecule, its adsorption capacity is often between that of linear PEI and branched PEI, limited by its molecular structure's loading density on the support. Hence, amine-impregnated adsorbents produced from diverse organic amine feedstocks manifest distinct advantages and deficiencies with respect to sorption capability, selectivity toward CO<sub>2</sub>, thermal regeneration demands, and long-term stability throughout direct air capture processes. When selecting organic amines to prepare supported amines suitable for direct air capture of CO<sub>2</sub>, it is necessary to comprehensively consider various factors in the actual application scenario, such as gas source composition, operating conditions, and cost. Through scientific and reasonable selection and optimization, the performance of supported amine adsorbents can be optimized.

## 2.2 Effect of Porous Supports

The impregnation method, as a common means of preparing impregnated supported amine adsorbents, relies on the unique physical properties of porous supports to achieve organic amine loading. Throughout the fabrication of impregnated amine-functionalized sorbents, the pore dimension distribution, surface area characteristics, along with surface chemical attributes of the support substrate exert a governing impact on their carbon dioxide capture behavior. In recent years, researchers have systematically investigated the CO<sub>2</sub> adsorption performance of supported amines by impregnating and loading different organic amines onto various porous supports, providing important basis for optimizing material design. Common porous supports include activated carbon, silica, bimetallic oxides, and metal-organic frameworks (MOFs).

Activated carbon possesses rich and diverse pore structures, encompassing micropores, mesopores, and macropores, and its specific surface area is considerable, often reaching 1000-3000 m<sup>2</sup>/g. The elaborated porous architecture and extensive surface area furnish abundant, uniformly dispersed anchoring locations for organic amine species. Activated carbon is typically prepared from carbon-rich raw materials, such as wood and coal, through a series of complex processes including carbonization and activation. Stemming from variations in precursor materials and synthetic approaches, its porous framework and surface chemistries diverge considerably, influencing amine incorporation levels and sorption characteristics. Hu Jingwei et al. used waste ion exchange resin as raw material, prepared a resin-based spherical activated carbon (HRSAC) through activation treatment, and then prepared an impregnated supported amine, PEI-HRSAC, by loading different masses of polyethyleneimine (PEI) onto its surface via the impregnation method. They experimentally analyzed the pore structure and adsorption performance of the activated carbon and the supported amine. Study results indicated that optimizing the activation technique permitted the constructed HRSAC to achieve a peak surface area of 1365 m<sup>2</sup>/g. When impregnated with 65% PEI (by mass, henceforth), the as-prepared PEI-HRSAC amine-functionalized material exhibited maximum CO<sub>2</sub> adsorption performance of 4.09 mmol/g at 75°C. Liu Liangying systematically studied the regulation of activated carbon pore structure, the preparation of supported amine adsorbents, and their CO<sub>2</sub> adsorption characteristics.

Siliceous substrates including SBA-15, MCM-41, and related variants represent frequently employed support matrices. Mesoporous silica features well-ordered pore channels, substantial pore dimensions, and elevated specific surface area, facilitating homogeneous dispersion of amine functionalities. The pore surfaces can be engineered to strengthen amine-support interactions and elevate the comprehensive performance of the resulting sorbent. Furthermore, mesoporous silica has good chemical stability, maintaining its own structure and properties under different DAC conditions. Holewinski et al. studied the correlation between CO<sub>2</sub> adsorption performance and organic amine morphology. PEI and mesoporous silica composites can effectively and reversibly adsorb CO<sub>2</sub>. The morphology of PEI inside silica affects carbon capture efficiency and rate. Small-angle neutron scattering disclosed that PEI first deposits a slender coating on internal pore surfaces, with supplementary quantities clustering into cylindrical plugs progressing along the channel axis. This framework corresponds with tendencies in amine utilization and pore dimension spectra, illuminating the equilibrium between reactive site availability and mass transfer accessibility. The instance of PEI deployed on hydrophobically engineered silica validates that such configurational approaches can boost CO<sub>2</sub> capacity and absorption velocity. Yan et al. constructed amorphous SiO<sub>2</sub>-Al<sub>2</sub>O<sub>3</sub> porous scaffolds with distinct surface acidities, thereafter generating supported amine materials via PEI solution impregnation, and evaluated CO<sub>2</sub> sorption behavior across assorted

temperatures, regeneration atmospheres, and humidity states. Data demonstrated that specimens with Si/Al ratios between 20 and 60 attained maximum uptake of 142.6 mg/g, whereas SiO<sub>2</sub>-Al<sub>2</sub>O<sub>3</sub> variants with Si/Al=5–50 displayed exceptional robustness under both arid and moisture-rich conditions. Moreover, they determined that the population of intermediate-strength Lewis acid locations on the SiO<sub>2</sub>-Al<sub>2</sub>O<sub>3</sub> exterior is essential for resisting urea formation, given that these positions facilitate substantial interlinking reactions between PEI and the substrate. This generates fresh understanding regarding the impact of silica support acid strength on solid amine capture material longevity.

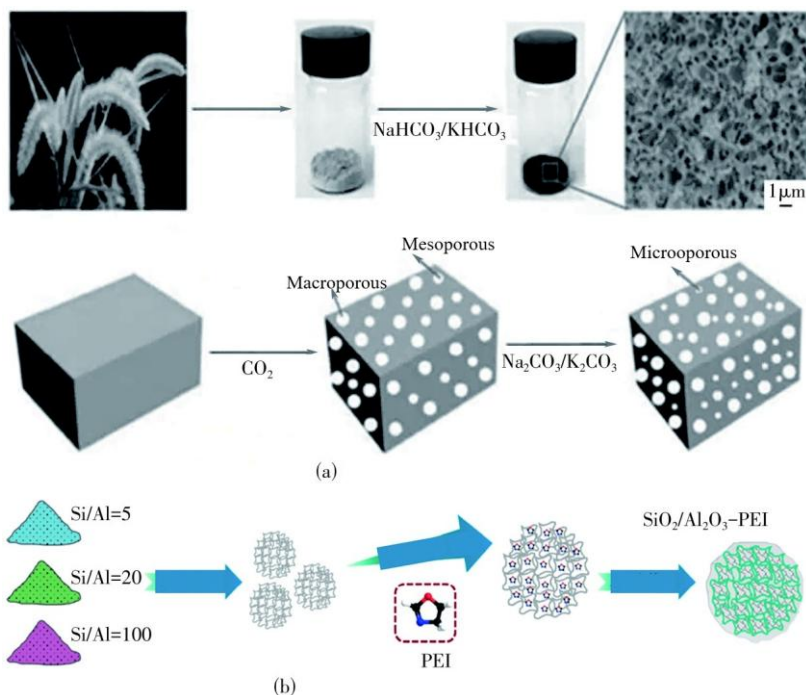


**Figure 5** Preparation process of carrier and solid amine [40,51]

Figure 5 shows the preparation process of activated carbon and PEI-impregnated SiO<sub>2</sub>/Al<sub>2</sub>O<sub>3</sub> supported amine. Alumina as a support has the prominent advantage of high mechanical strength and thermal stability. Under high temperature and high humidity environments, alumina can maintain the integrity of its own structure and stable chemical structure. This characteristic makes impregnated supported amine adsorbents using alumina as the support suitable for some adsorption processes with stringent temperature requirements, enabling stable CO<sub>2</sub> adsorption under high-temperature conditions. Chaikittisilp et al. prepared mesoporous  $\gamma$ -alumina-supported PEI composites as CO<sub>2</sub> adsorbents and evaluated their adsorption performance. In comparison to silica-supported amine materials, these sorbents exhibited greater capture capacity and amine utilization, particularly under atmospheric conditions. Additionally, this adsorbent preserved its integrity throughout repeated temperature swing tests and demonstrated superior durability upon steam contact, identifying it as a compelling option for CO<sub>2</sub> recovery systems employing steam stripping, especially for highly dilute gas sources. Sakwa-Novak and colleagues explored the structural changes in PEI-loaded  $\gamma$ -alumina adsorbents utilized for ambient air CO<sub>2</sub> extraction under steam exposure.

The adsorbent underwent CO<sub>2</sub> adsorption under DAC conditions and regeneration in flowing steam (5–24 h). Its equilibrium CO<sub>2</sub> capacity was evaluated under specific conditions, and physicochemical characterization was performed. Over a 12-hour period, the sorbent retained in excess of 90% of its original uptake capability (approximately 1.7 mmol/g). Following 24 hours, the capacity declined to 0.66 mmol/g attributable to PEI elution. Following steam exposure exceeding 90 minutes, the  $\gamma$ -alumina substrate underwent partial hydration, converting to boehmite. The phase transition was concentrated between 90 minutes and 12 hours, slowing down from 12 to 24 hours, and boehmite had little effect on PEI amine efficiency. This study further proved that  $\gamma$ -alumina/PEI supported amine is a promising adsorbent for DAC capture and steam regeneration.

Porous resins have unique physical and chemical properties, making them one of the ideal supports for preparing amine-functionalized solid adsorbents. Their pore structure is rich, pore size and distribution can be precisely controlled, and they have a large specific surface area, providing ample space for amine loading. Meng Yuan et al. loaded PEI onto porous resin HP20 via wet impregnation to prepare resin-based supported amine adsorption materials, investigating the effects of PEI loading, adsorption temperature, and pressure on their CO<sub>2</sub> adsorption performance. The results showed that the optimal PEI/adsorbent mass ratio was 50%. The material exhibited excellent adsorption performance under different CO<sub>2</sub> partial pressures, with an adsorption capacity of 3.06–3.78 mmol/g at 30°C, and CO<sub>2</sub>/CH<sub>4</sub> and CO<sub>2</sub>/N<sub>2</sub> selectivity were at a high level in the 2–100 kPa pressure range. Hu Jingwei et al. used spherical waste ion exchange resin as raw material, prepared HRSAC through CO<sub>2</sub> activation and acid washing, and then obtained the adsorption material PEI-HRSAC by loading PEI. The investigation revealed that subsequent to activation at 950°C for 60 minutes followed by acid leaching, HRSAC exhibited a surface area of 1365 m<sup>2</sup>/g, mesoporous volume of 2.04 cm<sup>3</sup>/g, and aperture dimensions ranging 10–40 nm. The CO<sub>2</sub> capture behavior of PEI-HRSAC exhibited an initial rise followed by a decline as both temperature and PEI loading increased. With 65% PEI loading at 75°C, the sorption capacity reached its maximum of roughly 4.09 mmol/g. After four thermal cycles, the material maintained 3.66 mmol/g, reflecting satisfactory regeneration stability. Metal-organic frameworks (MOFs) consist of metal ions or clusters coordinated with organic bridging ligands to form crystalline porous architectures. featuring exceptionally high surface area, tunable pore dimensions, and plentiful accessible active centers. Through rational design of structure and selection of linkers, amino groups can be introduced into the framework or pores to prepare high-performance amine-functionalized MOF adsorbents. Rim et al. assembled amine-supported adsorbents by infusing tetraethylenepentamine (TEPA) into two distinct carriers [commercial  $\gamma$ -Al<sub>2</sub>O<sub>3</sub> and MIL-101(Cr)], and investigated the CO<sub>2</sub> capture mechanisms on these TEPA-functionalized materials via in-situ infrared spectroscopy. The results indicated that on TEPA-MIL-101(Cr), weak chemisorption (carbamic acid formation) was primary; in contrast, on TEPA- $\gamma$ -Al<sub>2</sub>O<sub>3</sub>, strong chemisorption (carbamate formation) occurred preferentially. Under humid conditions, the development of both carbamic acid and carbamate species on TEPA-containing sorbents was augmented, with atmospheric moisture generating the strongest effect. This study is of great significance for deeply understanding the interaction mechanism between MOF-based supported amines and CO<sub>2</sub>, providing a theoretical basis for optimizing DAC adsorbent performance. Because MOF structures are adjustable, using them as amine carriers is a general method for preparing effective amine adsorbents. Darunte and colleagues analyzed the effectiveness of amine-infused MIL-101(Cr) for capturing CO<sub>2</sub> from simulated air, incorporating two different amines, TREN and PEI-800, into MOF cavities at various concentrations. Findings revealed that MIL-101(Cr)-TREN delivered considerable CO<sub>2</sub> uptake at elevated TREN loading, yet pronounced amine degradation occurred throughout successive temperature swing operations. MIL-101(Cr)-PEI-800 manifested enhanced cyclic resilience. Employing amine efficiency as a performance metric, this indicator varied substantially with PEI-800 concentration. At impregnation levels of 1–1.1 mmol/gMOF, MIL-101(Cr)-PEI-800 struck an effective balance between CO<sub>2</sub> sorption capacity and kinetic behavior. Table 1 summarizes the performance parameters of impregnated DAC supported amines reported in recent years.

**Table 1** Adsorption Performance of Impregnated DAC Supported Amines

Support Material	Organic Amine	Amine Loading (Mass Fraction)	Adsorption Capacity / mmol·g <sup>-1</sup>	Adsorption Conditions	Desorption Conditions	Stability	Reference
SBA-15	PEI	50%	1.55	30°C, dry, CO <sub>2</sub> 400 ppm	110°C, He purge		[50]
SBA-15	PEI	75%	1.12	25°C, dry, CO <sub>2</sub> 400 ppm	110°C, N <sub>2</sub> purge	5.5% capacity decay after 10 cycles	[37]
SBA-15	PPI	45%	1.35	35°C, dry, CO <sub>2</sub> 400 ppm	70°C, N <sub>2</sub> purge	Capacity stabilized after 4 cycles	[61]
SBA-15	PPI	50%	1.0	35°C, dry, CO <sub>2</sub> 400 ppm	110°C, He purge	Almost no capacity decay after 20 cycles	[41]
SBA-15	PPI	14 mmol/g	1.25	25°C, dry, CO <sub>2</sub> 400 ppm	110°C, N <sub>2</sub> purge	Almost no capacity decay after 50 cycles	[62]

Support Material	Organic Amine	Amine Loading (Mass Fraction)	Adsorption Capacity / mmol·g <sup>-1</sup>	Adsorption Conditions	Desorption Conditions	Stability	Reference
SBA-15	PGA	15%~45%	0.6	25°C, dry, CO <sub>2</sub> 400 ppm	110°C, N <sub>2</sub> purge	10.9% capacity decay after 20 cycles	[63]
SBA-15	PPG	50%	0.6	30°C, dry, CO <sub>2</sub> 400 ppm	120°C, He purge	54.5% capacity decay after 5 cycles	[64]
SBA-15	Ph-3-ED	60%	1.4	25°C, humid, CO <sub>2</sub> 400 ppm, RH 30%	110°C, He purge	Capacity stabilized after 25 cycles	[65]
SBA-15	PEI	30%	0.19	25°C, dry, CO <sub>2</sub> 400 ppm	110°C, Ar purge	41.2% capacity decay after 4 cycles	[46]
Al-SBA-15	PEI	34%	0.29	25°C, dry, CO <sub>2</sub> 400 ppm	110°C, Ar purge	—	[46]
Ti-SBA-15	PEI	32%	0.64	25°C, dry, CO <sub>2</sub> 400 ppm	110°C, Ar purge	6% capacity decay after 4 cycles	[46]
Ce-SBA-15	PEI	33%	0.68	25°C, dry, CO <sub>2</sub> 400 ppm	110°C, Ar purge	—	[46]
Zr-SBA-15	PEI	35%	0.85	25°C, dry, CO <sub>2</sub> 400 ppm	110°C, Ar purge	Capacity stabilized after 4 cycles	[46]
Zr-SBA-15	PEI	50%	1.05	30°C, dry, CO <sub>2</sub> 400 ppm	110°C, N <sub>2</sub> purge	—	[46]
EtSNT	PEI	33%	1.0	25°C, dry, CO <sub>2</sub> 400 ppm	100°C, N <sub>2</sub> purge	Capacity stabilized after 8 cycles	[46]
SBA-15	TEPA	50%	2.3	25°C, dry, CO <sub>2</sub> 400 ppm	110°C, N <sub>2</sub> purge	2.8% capacity decay after 10 cycles	[37]
MCF pellets	PEI	68%	1.94	46°C, dry, CO <sub>2</sub> 420 ppm	81°C, N <sub>2</sub> purge	—	[66]
MCF pellets	PEI	68%	2.52	46°C, humid, CO <sub>2</sub> 420 ppm, H <sub>2</sub> O 20 ml/L	81°C, N <sub>2</sub> purge	—	[66]
Hierarchical silica	PEI	2.62 g/g	2.6	30°C, dry, CO <sub>2</sub> 400 ppm	110°C, He purge	Capacity stabilized after 5 cycles	[67]
Hierarchical silica	PEI	2.62 g/g	3.36	30°C, humid, CO <sub>2</sub> 400 ppm, RH 19%	110°C, He purge	18.15% capacity decay after 5 cycles	[67]
AHTSA	PEI	10%	1.64	25°C, CO <sub>2</sub> 400 ppm	130°C, N <sub>2</sub> purge	Capacity stabilized after 15 cycles	[68]
Fumed silica	PO-PEHA	50%	2.25	25°C, humid, CO <sub>2</sub> 1000 ppm, RH 50%	50°C, CO <sub>2</sub> purge, 400 ppm	Capacity stabilized after 5 cycles	[69]
Fumed silica	PO-TEPA	50%	2.0	25°C, humid, CO <sub>2</sub> 1000 ppm, RH 50%	50°C, CO <sub>2</sub> purge, 400 ppm	Capacity stabilized after 45 cycles	[69]
Fumed silica	HBPG	50%	0.80	25°C, humid, CO <sub>2</sub> 400 ppm, RH 35%	100°C, N <sub>2</sub> purge	—	[70]
Mesoporous carbon	PEI	60%	2.25	25°C, dry, CO <sub>2</sub> 400 ppm	110°C, N <sub>2</sub> purge	Capacity stabilized after 10 cycles	[71]
Carbon nanotubes	PEI	10%	1.07	25°C, dry, CO <sub>2</sub> 3500 ppm	80°C, vacuum	—	[72]
γ-Alumina	PEI	48%	1.74	25°C, dry, CO <sub>2</sub> 400 ppm	110°C, steam purge	Capacity stabilized after 3 cycles	[53]
γ-Alumina	PEI	7.95 g/g	1.96	30°C, dry, CO <sub>2</sub> 400 ppm	110°C, steam purge	—	[54]
Alumina monolith	PEI	0.44 g/g	0.9	30°C, dry, CO <sub>2</sub> 400 ppm	110°C, steam purge	14% capacity decay after 5 cycles	[73]
Halloysite nanotubes	PEI	40%	1.25	25°C, dry, CO <sub>2</sub> 400 ppm	80°C, vacuum	3.28% capacity decay after 50 cycles	[74]
Zeolite Y	TEPA	10%	1.12	25°C, CO <sub>2</sub> 5000 ppm	100°C, N <sub>2</sub> purge	Capacity stabilized after 5 cycles	[75]

Support Material	Organic Amine	Amine Loading (Mass Fraction)	Adsorption Capacity / mmol·g <sup>-1</sup>	Adsorption Conditions	Desorption Conditions	Stability	Reference
NPEI-SIPs	PEI	49%	1.7	50°C, dry, CO <sub>2</sub> 400 ppm	120°C, N <sub>2</sub> purge	7.8% capacity decay after 20 cycles	[76]
Resin HP2MGL	PEI	50%	2.13	25°C, dry, CO <sub>2</sub> 5000 ppm	100°C, N <sub>2</sub> purge	Capacity stabilized after 5 cycles	[77]
Resin HP2MGL	PEI	50%	3.04	25°C, humid, CO <sub>2</sub> 500 ppm, RH 40%	100°C, N <sub>2</sub> purge	Capacity stabilized after 5 cycles	[77]
Resin HP20	PEI	50%	2.26	25°C, dry, CO <sub>2</sub> 400 ppm	100°C, N <sub>2</sub> purge	Almost no capacity decay after 5 cycles	[78]
Resin MR10	PEI	50%	2.64	25°C, dry, CO <sub>2</sub> 1000 ppm	70°C, N <sub>2</sub> purge	10.6% capacity decay after 3 cycles	[79]
Resin MR10	PEI	50%	2.92	25°C, humid, CO <sub>2</sub> 1000 ppm, RH 50%	70°C, N <sub>2</sub> purge		[79]
Resin KBS	PEI	20%	1.59	20°C, humid, CO <sub>2</sub> 4000 ppm, H <sub>2</sub> O 15.6 ml/L	50°C, N <sub>2</sub> purge	—	[80]
MIL-101(Cr)	PEI	60%	1.04	25°C, dry, CO <sub>2</sub> 400 ppm	110°C, He purge	4.6% capacity decay after 3 cycles	[60]
MIL-101(Cr)	PEI	50%	1.17	-20°C, dry, CO <sub>2</sub> 400 ppm	60°C, He purge	Capacity stabilized after 15 cycles	[25]
MIL-101(Cr)	TREN	45%	2.76	25°C, dry, CO <sub>2</sub> 400 ppm	110°C, He purge	15.1% capacity decay after 3 cycles	[60]
MIL-101(Cr)	TEPA	30%	0.72	-20°C, dry, CO <sub>2</sub> 400 ppm	25°C, He purge	30% capacity decay after 15 cycles	[25]
PEI-Mg0.55Al-O	PEI	67%	1.66	25°C, dry, CO <sub>2</sub> 400 ppm	120°C, N <sub>2</sub> purge	—	[43]
PEI-Mg0.55Al-O	PEI	67%	2.27	25°C, humid, CO <sub>2</sub> 400 ppm	120°C, N <sub>2</sub> purge	2.7% capacity decay after 20 cycles	[43]
TEPA-Mg0.55Al-O	TEPA	67%	3.0	25°C, dry, CO <sub>2</sub> 400 ppm			

### 3 Grafted Supported Amines

The feeble bonding between amine species and the substrate in impregnated sorbents results in comparatively inferior stability throughout thermal cycling regeneration. To address this, researchers have developed grafted supported amine adsorbents through covalent chemical bonds. Grafting is predominantly achieved through silanization processes involving aminosilanes and surface hydroxyl functionalities, though instances employing cross-coupling methodologies have additionally been documented.

#### 3.1 Effect of Amine Type

A wide variety of aminosilanes—including aminomethyl (C1), 2-aminoethyl (C2), 3-aminopropyl (APS), 4-aminobutyl (C4), 5-aminopentyl (C5), N-methylaminopropyl (MAPS), N-butylaminopropyl (NBAPS), 3-amino-3-methylbutyl (AMBS), tert-butylaminopropyl (TBAPS), N-cyclohexylaminopropyl (CHAPS), N-phenylaminopropyl (PHAPS), N,N-dimethylaminopropyl (DMAPS), 3-(2-aminoethylamino)propyl (DI), 3-(2-aminopropylamino)propylsilane (L-propyl), N,N'-bis(3-trimethoxysilylpropyl)urea (UREA), 3-[2-(2-aminoethylamino)ethylamino]propyl (TRI), 3-(2-aminoethylamino)methylsilane (CH2DETA), bis(2-aminoethyl)amine (B-ethyl), bis(2-aminopropyl)amine (B-propyl), and tris(2-aminoethyl)amine (TREN)—have been tested for capturing carbon from gases with very low CO<sub>2</sub> levels. Because of entropic effects, primary amines are more efficient than secondary and tertiary amines, which explains why APS is widely used for capturing carbon at extremely low concentrations. The flexible propyl chain in APS allows two nearby amine groups to work together to capture one CO<sub>2</sub> molecule, but longer chains do not provide extra benefits. However, APS-grafted adsorbents have low nitrogen content (usually under 5 mmol/g), which limits how much CO<sub>2</sub> uptake capacity can be improved in supported amine systems.

To achieve higher amine loading, aminosilanes containing multiple amino groups are used for grafting. For example, monolayer-grafted TRI on SBA-15 and pore-expanded MCM-41 (PE-MCM-41) achieved amine loadings of 6.0 mmol/g and 6.2 mmol/g, respectively. These materials displayed decent CO<sub>2</sub> uptake ability and fairly rapid kinetics in DAC operations at intermediate to high loadings, with enhanced capture under wet conditions. By comparison, diamines underperformed, likely because secondary amine functionalities are not fully available. Such groups could be sterically impeded by chemisorbed CO<sub>2</sub> or hydrogen-bonded to silanol surface groups [Fig. 6(a), (b)]. Of late, various branched and linear aminosilanes joined by ethyl or propyl bridges have been investigated [Fig. 6(c)]. Adsorbents grafted with branched silanes bearing dual primary amine terminations (B-ethyl, B-propyl) showed amine efficiency on a par with APS and greater than linear analogues (DI and L-propyl). Yet linear silanes enable dense functionalization under water-free conditions, reaching incorporations beyond 1.7 mmol/g, whereas branched silane loading is restricted under 1.3 mmol/g [Fig. 6(d), (e)]. All derivatized sorbents kept good thermal stability, and neighboring amino units linked through propyl connectors achieved better oxidative resilience.

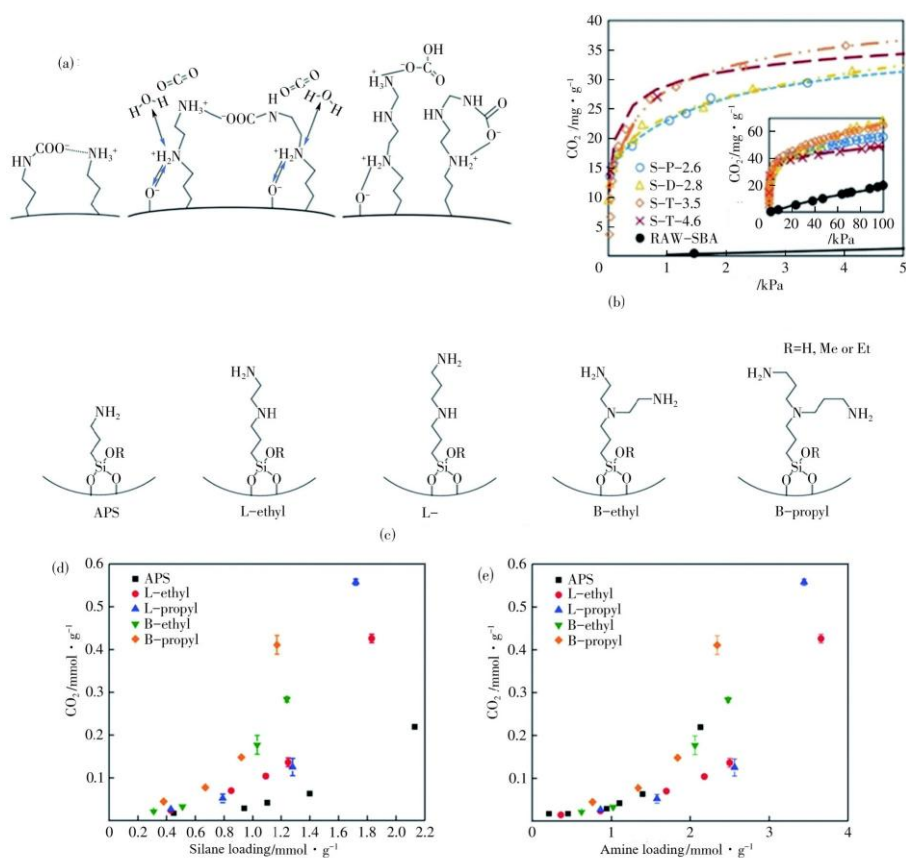


**Figure 6** Amine types and their impacts

In primary and secondary amines on supports, carbamate salts are preferentially formed as the chemisorbed CO<sub>2</sub> species, requiring two amino groups to bind one CO<sub>2</sub> molecule. Ammonium bicarbonate generation avoids this cross-linking effect, which may aggravate CO<sub>2</sub> diffusion limitations, by coordinating to one nitrogen atom. Forming ammonium bicarbonate can also reduce the energy needed for regeneration, since they are less thermally stable than carbamates. Spectroscopic studies have found ammonium bicarbonate in every type of amine. Tertiary amines—which form only ammonium bicarbonate—may be more efficient than primary and secondary amines. However, they react slowly, and even using tertiary amines for surface modification under humid conditions gives poor adsorption results. Recently, three sterically hindered amines—one primary (AMBS) and two secondary (CHAPS and TBAPS)—were tested for DAC (Fig. 7). These prefer to form weakly-bound ammonium bicarbonate under moist conditions while keeping fast CO<sub>2</sub> adsorption rates. AMBS was also stable after accelerated oxidation tests. But the CO<sub>2</sub> capacity of solids with these bulky amines is much lower than in

solution. This difference could be explained by studying how solvation and hydrogen bonding affect chemisorbed CO<sub>2</sub>.

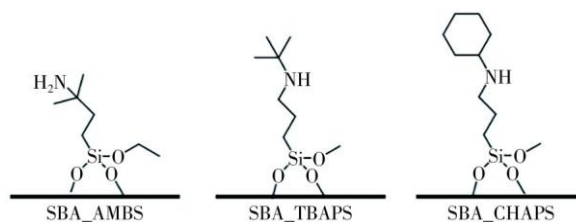
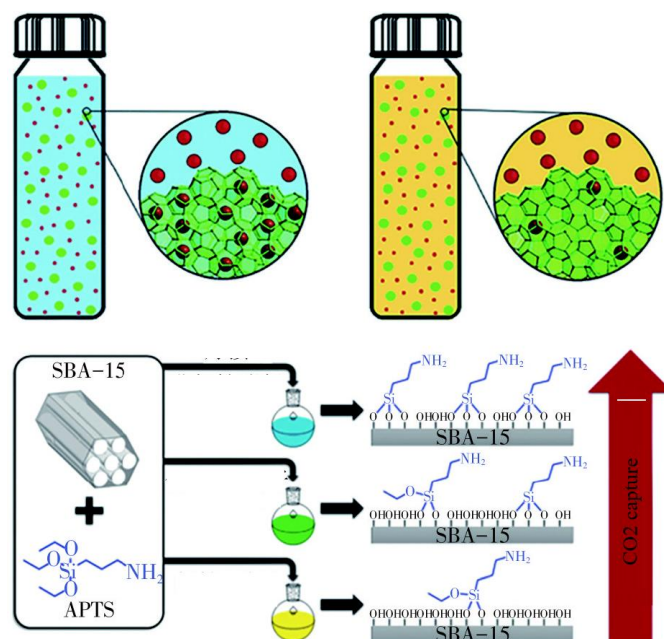


Figure 7 Structure of aminosilane with steric hindrance [87]

### 3.2 Effect of Grafting Method

Conducting multilayer amine grafting in water-containing systems provides a way to boost amine loading by overcoming the constraint of limited hydroxyl groups on the support surface. This process, termed wet grafting, involves pre-wetting the porous carrier by adding water to the dispersion (such as toluene), then attaching the aminosilane to the surface under heating. Belmabkhout et al. showed that wet-grafted TRI on PE-MCM-41 obtained 7.9 mmol/g amine loading and 0.98 mmol/g adsorption capacity at 25°C and 400 ppm CO<sub>2</sub>. This material also demonstrated good hydrothermal stability in steam regeneration experiments. Since then, wet grafting has been broadly adopted for other mesoporous supports like SBA-15, alumina, KIT-6, and hierarchical bimodal mesoporous silica (HBS). Commercial silica gel was once viewed as having unsatisfactory performance in DAC; however, remarkably, after wet grafting, it achieved CO<sub>2</sub> capacities of 0.773 mmol/g and 1.098 mmol/g under dry and humid conditions, respectively. Such very high amine loading cannot be explained by silanization between hydrolyzed alkoxy groups of amine molecules and surface hydroxyl groups (which produces only monolayer grafting). Actually, surface water accelerates hydrolysis of unreacted alkoxy groups and supplies additional hydroxyl groups for multilayer aminosilane coating through Si-O-Si bridges. Water presence also greatly shortens grafting time (to under 30 minutes), likely due to formation of highly reactive silanol groups from aminosilane alkoxy groups. So far, toluene is the most commonly used solvent in the aminosilane grafting process. Recent studies have shown that solvent properties can also greatly affect the surface configuration of supported amines. A typical example is alkylamine-grafted MIL-101. While possessing a highly porous structural matrix coupled with outstanding robustness under extreme conditions, the material demonstrates only moderate CO<sub>2</sub> capture performance. Simply substituting the grafting solvent—from dichloromethane to cyclohexane—led to over a 100% enhancement in CO<sub>2</sub> adsorption for amine-modified MIL-101(Cr), together with improved CO<sub>2</sub>/N<sub>2</sub> selectivity. Such augmentation is presumably attributed to lower solvent polarity, which diminishes interactions with amine groups and thus elevates grafting efficiency (Fig. 8). Further deliberate explorations assessed three apolar solvents, two polar aprotic solvents, and three polar protic solvents, manifesting a marked reliance of supported amine behavior on solvent polarity characteristics. In particular, the CO<sub>2</sub> sorption capability and amine effectiveness of functionalized materials are determined by the interplay between support and solvent. Among apolar options, cyclohexane exceeded both hexane and toluene, enabling nitrogen content (by mass) to reach 5.21% while securing a stable surface configuration. These studies indicate that enhancing the performance of grafted supported amines through rational solvent selection is feasible.



**Figure 8** The interface between alkylamine solution and MIL-101(Cr) [92], as well as the possible connection configurations for amine grafting using non-polar, dipolar-apolar, and polar-protonic solvents, and their CO<sub>2</sub> adsorption capabilities [102]

Although conventional solvent-based grafting remains prevalent in industrial material synthesis, it inevitably produces substantial solvent waste and triggers unwanted oligomerization side reactions. Supercritical carbon dioxide (scCO<sub>2</sub>) offers a sustainable alternative that enhances amine precursor diffusion and enables efficient surface functionalization. The process typically operates at 40–60°C under 12.5–20.0 MPa for 2–3 hours, with CO<sub>2</sub> subsequently recovered through pressure reduction. Since scCO<sub>2</sub> readily reacts with primary and secondary amines to generate carbamate species, alcohol co-solvents are introduced to dissolve the alkylammonium byproducts. Studies demonstrate that diamine-grafted SBA-15 can be synthesized using scCO<sub>2</sub> containing 10 mol% ethanol or pure ethanol at 50°C and 12.5 MPa, delivering an amine efficiency of 0.4 at 25°C—markedly exceeding the below-0.1 values obtained via conventional toluene-based protocols. This superior performance originates from unimpeded CO<sub>2</sub> diffusion within the functionalized matrix until amine loadings approach 3 mmol/g.

Silica supports featuring three-dimensional interconnected mesoporous frameworks exhibit considerable promise for surface amine immobilization and enhanced CO<sub>2</sub> transport during adsorption. Chaffee et al. demonstrated that aminosilane-grafted hexagonal mesoporous silica (HMS) with wormhole-like structures achieved high amine efficiency (~0.69) for post-combustion carbon capture. Recently, tailored HMS variants have been deployed for direct air capture applications. Employing dodecylamine (C<sub>12</sub> chain) as a template, followed by calcination removal, yielded an optimal HMS pore structure that maintained CO<sub>2</sub> accessibility even at 5.4 mmol/g amine loading. However, the narrow pore dimensions of HMS (2.5–2.9 nm) constrain multilayer grafting strategies aimed at higher loadings. In contrast, hierarchical bimodal mesoporous silica (HBS) possessing dual interconnected cylindrical pores (~9.1 nm and 33.8 nm) proved highly effective as a support, allowing deep aminosilane penetration and uniform amine dispersion. Wet-grafted HBS retained greater mesopore accessibility at high functionalization densities and exhibited reduced kinetic limitations compared to wet-grafted SBA-15. Under dry air feed at 3000 h<sup>-1</sup> space velocity, this material demonstrated an impressive CO<sub>2</sub> adsorption capacity of 1.04 mmol/g.

### 3.3 Effect of Porous Supports

The effective synthesis of grafted supported amines relies on supports with high specific surface area, tunable pore structure, and abundant surface hydroxyl groups. Most grafted supported amines use ordered mesoporous silica as the support, such as MCM-41, SBA-15, and their derivatives. These materials offer well-defined pore geometries, exceptional thermal stability, and facile surface modification chemistry. The silanol density on silica

surfaces critically influences grafting density and amine distribution, with higher hydroxyl concentrations generally promoting greater amine loading. However, excessive amine immobilization can lead to pore blockage and reduced accessibility for CO<sub>2</sub> molecules. Consequently, balancing amine loading with textural preservation remains essential for optimizing capture performance. Recent advances have explored hybrid organic-inorganic supports and surface activation protocols to enhance grafting efficiency while maintaining structural integrity. Post-synthetic treatments including thermal annealing and controlled hydration further modulate the surface chemistry and amine accessibility, thereby influencing the overall CO<sub>2</sub> sorption kinetics and capacity. The successful fabrication of amine-grafted solid sorbents depends critically on support materials possessing elevated specific surface areas, adjustable porous architectures, and plentiful surface hydroxyl functionalities. Ordered mesoporous silicas dominate this application domain, encompassing MCM-41, SBA-15, and related structural analogues. These substrates provide precisely engineered pore geometries, outstanding thermal resistance, and readily modifiable surface chemistry. Silanol group density on silica surfaces plays a pivotal role in determining grafting efficiency and amine spatial distribution, where elevated hydroxyl concentrations typically facilitate increased amine incorporation. Nevertheless, excessive functionalization risks pore constriction and compromised CO<sub>2</sub> accessibility. Therefore, striking an optimal equilibrium between amine loading and textural retention proves vital for maximizing capture effectiveness. Emerging research directions include hybrid organic-inorganic frameworks and advanced surface activation methodologies to boost grafting yields without sacrificing structural robustness. Supplementary post-synthetic modifications such as controlled thermal treatment and hydration management additionally tune surface characteristics and amine availability, consequently governing overall CO<sub>2</sub> uptake kinetics and saturation capacity.

Pore-expanded variants including MCM-41, MCM-48, SBA-15, KIT-6, and MCF have attracted particular attention. Elucidating how silica support porosity impacts amine immobilization and subsequent CO<sub>2</sub> capture behavior remains fundamentally important. Pore-enlarged MCM-41 specifically benefits from expanded aperture dimensions and enhanced void volumes, enabling superior amine dispersion and facilitated gas diffusion throughout the porous network. The successful fabrication of amine-grafted solid sorbents depends critically on support materials possessing elevated specific surface areas, adjustable porous architectures, and plentiful surface hydroxyl functionalities. Ordered mesoporous silicas dominate this application domain, encompassing MCM-41, SBA-15, and related structural analogues. These substrates provide precisely engineered pore geometries, outstanding thermal resistance, and readily modifiable surface chemistry. Silanol group density on silica surfaces plays a pivotal role in determining grafting efficiency and amine spatial distribution, where elevated hydroxyl concentrations typically facilitate increased amine incorporation. Nevertheless, excessive functionalization risks pore constriction and compromised CO<sub>2</sub> accessibility. Therefore, striking an optimal equilibrium between amine loading and textural retention proves vital for maximizing capture effectiveness. Emerging research directions include hybrid organic-inorganic frameworks and advanced surface activation methodologies to boost grafting yields without sacrificing structural robustness. Supplementary post-synthetic modifications such as controlled thermal treatment and hydration management additionally tune surface characteristics and amine availability, consequently governing overall CO<sub>2</sub> uptake kinetics and saturation capacity.

Pore-expanded variants including MCM-41, MCM-48, SBA-15, KIT-6, and MCF have attracted particular attention. Elucidating how silica support porosity impacts amine immobilization and subsequent CO<sub>2</sub> capture behavior remains fundamentally important. Pore-enlarged MCM-41 specifically benefits from expanded aperture dimensions and enhanced void volumes, demonstrating enhanced CO<sub>2</sub> sorption capacity and accelerated uptake kinetics at trace concentrations following organic amine functionalization. Similar phenomena have been observed for SBA-15, especially under wet grafting conditions, where small pores can lead to significant pore blockage and reduce amine accessibility. According to Anyanwu et al., TRI molecules on wet-grafted SBA-15 exhibited aggregation. After expanding the pore size of SBA-15 from 8 nm to 12.3 nm by adding methyl isobutyl ketone during synthesis, the aggregation phenomenon was eliminated, achieving higher adsorption capacity. The fabrication of high-performance amine-functionalized solid sorbents necessitates support materials with considerable specific surface areas, tunable porous structures, and abundant surface hydroxyl groups. Ordered mesoporous silicas represent the primary class of supports utilized, including MCM-41, SBA-15, and analogous structural variants. These materials offer precisely controlled pore geometries, excellent thermal stability, and flexible surface modification chemistry. The density of silanol groups on silica surfaces critically determines grafting efficiency and amine distribution, with higher hydroxyl concentrations typically favoring increased amine loading. However, excessive functionalization can lead to pore blockage and hinder CO<sub>2</sub> accessibility. Therefore,

achieving an optimal balance between amine loading and structural preservation is crucial for maximizing capture performance. Emerging research explores hybrid organic-inorganic supports and advanced surface activation methods to enhance grafting efficiency without compromising structural integrity. Additional post-synthetic treatments, such as controlled thermal annealing and humidity regulation, further adjust surface properties and amine accessibility, thereby influencing overall CO<sub>2</sub> adsorption kinetics and capacity. Pore-expanded versions of MCM-41, MCM-48, SBA-15, KIT-6, and MCF have attracted considerable attention. Understanding how the pore structure of silica supports affects amine grafting and subsequent CO<sub>2</sub> capture performance is essential. Pore-expanded MCM-41, with its larger pore size and volume, shows improved CO<sub>2</sub> adsorption capacity and faster kinetics at very low concentrations after amine functionalization. However, under direct air capture conditions with high gas flow rates, wet-grafted pore-expanded SBA-15 exhibited breakthrough CO<sub>2</sub> capacities below 0.15 mmol/g, indicating significant diffusion limitations. Ordered mesoporous silicas are synthesized through the polymerization of silica precursors around organic templates (structure-directing agents), followed by template removal to create the desired porous structure. Template removal is commonly performed via high-temperature calcination in air, but prolonged heating can cause dehydroxylation, reducing the silanol density available for grafting. Although milder template removal methods have been proposed, such as solvent extraction and glow discharge plasma, these are often expensive, time-consuming, or ineffective at completely removing organic templates. Recently, ionic liquids (ILs) have been successfully used to extract P123 templates from as-synthesized SBA-15 at 120°C (Fig. 9). The IL-treated SBA-15 retained silanol densities above 5.1 OH/nm<sup>2</sup>, significantly higher than the 3.0 OH/nm<sup>2</sup> observed in calcined SBA-15. Furthermore, both the organic template and the IL can be recovered and reused, demonstrating practical feasibility. After grafting, the IL-treated SBA-15 showed a 51% increase in amine loading compared to conventionally treated samples, and its CO<sub>2</sub> capacity in DAC applications increased nearly threefold. The mechanism of IL treatment involves disrupting hydrogen bonds between surface silanol groups and the ethylene oxide (EO) groups of the P123 template, similar to the dissolution of cellulose by ILs. Future research combining optimized pore structure design, improved template removal methods, and wet grafting techniques can further enhance the CO<sub>2</sub> adsorption performance of ordered mesoporous silicas at very low concentrations.

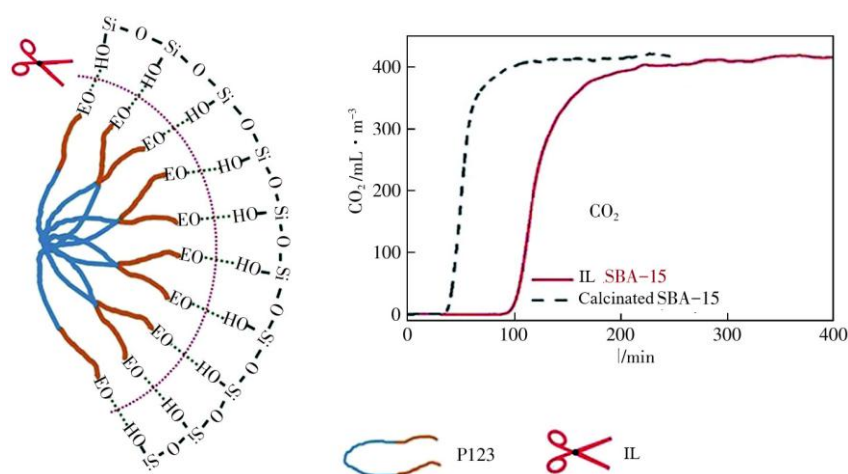


**Figure 9** Principle of removing amine grafting template through ionic liquid treatment [84]

The current batch synthesis of ordered mesoporous silica is characterized by poor efficiency and elevated expenses, motivating exploration of substitute support materials. Naturally sourced nanofibrillated cellulose (NFC) stands out as an attractive alternative, boasting plentiful hydroxyl moieties distributed across its carbohydrate framework. Experimental results demonstrate that NFC modified with diamine (DI) retained a steady CO<sub>2</sub> working capacity near 0.695 mmol/g across 20 direct air capture cycles, declining merely 5% following 100 humid operational cycles. Mesoporous  $\gamma$ -alumina additionally qualifies as a grafting-appropriate support, exhibiting enhanced hydrothermal robustness relative to silica matrices and consequently preserving structural coherence throughout extended steam regeneration protocols. Upon wet grafting with (3-aminopropyl)triethoxysilane (APS) at 2.92 mmol/g,  $\gamma$ -alumina realized an uptake of 0.79 mmol/g at ambient temperature (25°C) and 400 ppm CO<sub>2</sub> concentration. The

inherent alkalinity of alumina potentially participates in CO<sub>2</sub> binding, while in-situ FTIR characterization indicates that under conditions of extreme CO<sub>2</sub> dilution coupled with dense amine functionalization, amine-derivatized alumina engages an adsorption mechanism comparable to silica-based analogues. Table 2 catalogues the capture performance metrics of grafted supported amines reported in contemporary literature.

**Table 2** Adsorption Performance of Grafted DAC Supported Amines

Adsorbent	Adsorption Capacity / mmol·g <sup>-1</sup>	Adsorption Conditions	Desorption Conditions	Adsorption Heat / kJ·mol <sup>-1</sup>	Stability	Reference
(N <sub>2</sub> H <sub>4</sub> )1.8-Mg <sub>2</sub> (dobdc)	3.89	Volumetric, 25°C, dry, CO <sub>2</sub> 400 ppm	He purge, 130°C	80	Almost no capacity decay after 5 cycles (adsorption at 15% CO <sub>2</sub> )	[116]
en-Mg <sub>2</sub> (dobdc)	1.51	Gravimetric, 25°C, dry, CO <sub>2</sub> 400 ppm	Vacuum, 120°C	—	Almost no capacity decay after 4 cycles	[117]
en-Mg <sub>2</sub> (dobpdc)	2.83	Volumetric, 25°C, dry, CO <sub>2</sub> 390 ppm	Ar purge, 150°C	51	4% capacity decay after 20 cycles	[118]
m <sub>men</sub> -Mg <sub>2</sub> (dobpdc)	2.0	Volumetric, 25°C, dry, CO <sub>2</sub> 390 ppm	N <sub>2</sub> purge, 120°C	71	Almost no capacity decay after 10 cycles	[119]
m <sub>men</sub> -Mg <sub>2</sub> (dobpdc)	2.25	Volumetric, 25°C, dry, CO <sub>2</sub> 390 ppm	N <sub>2</sub> purge, 120°C	73	1.9% capacity decay after 30 cycles	[20]
epn-Mg <sub>2</sub> (dobpdc)@PDMS	2.27	IR, 25°C, humid, CO <sub>2</sub> 1000 ppm, RH 98%	N <sub>2</sub> purge, 70°C	-	Almost no capacity decay after 10 cycles	[120]
epn-Mg <sub>2</sub> (dobpdc)@PDVF	1.85	Volumetric, 25°C, dry, CO <sub>2</sub> 1000 ppm	N <sub>2</sub> purge, 150°C	64	Almost no capacity decay after 10 cycles; Almost no decay after 4 weeks at 25°C, RH 60%	[121]
epn-Mg <sub>2</sub> (dobpdc)@SBS	1.79	Volumetric, 25°C, dry, CO <sub>2</sub> 1000 ppm	N <sub>2</sub> purge, 130°C	-	Almost no capacity decay after 10 cycles; Almost no decay after 30 days at 25°C, RH 60%	[22]
Zn-OH	2.45	Volumetric, 27°C, dry, CO <sub>2</sub> 400 ppm	N <sub>2</sub> purge, 100°C	71	Almost no capacity decay after 10 cycles	[122]
Ni-OH	2.70	Volumetric, 27°C, dry, CO <sub>2</sub> 400 ppm	N <sub>2</sub> purge, 150°C	84	Almost no capacity decay after 5 cycles	[123]
Co-OH	2.0	Volumetric, 27°C, dry, CO <sub>2</sub> 400 ppm	N <sub>2</sub> purge, 150°C	68		[123]
Pri-SBA-15	0.50	Gravimetric, 25°C, humid, CO <sub>2</sub> 400 ppm, RH 23%	N <sub>2</sub> purge, 90°C	-	Almost no capacity decay after 2 cycles	[95]
Dia-SBA-15	0.30	Gravimetric, 25°C, humid, CO <sub>2</sub> 400 ppm, RH 23%	N <sub>2</sub> purge, 90°C	—		[95]
Tri-SBA-15	0.48	Gravimetric, 25°C, humid, CO <sub>2</sub> 400 ppm, RH 23%	N <sub>2</sub> purge, 90°C	-	Almost no capacity decay after 2 cycles	[95]
TRI-PE-MCM-41	0.98	Volumetric, 25°C, dry, CO <sub>2</sub> 400 ppm	He purge, 150°C	-	3.77% capacity decay after 6 cycles (adsorption at 1000 ppm CO <sub>2</sub> )	[124]
TRI-PE-MCM-41	0.81	Volumetric, 25°C, dry, CO <sub>2</sub> 400 ppm	N <sub>2</sub> purge, 120°C	92	0.9% capacity decay after 30 cycles	[20]
TRI-WG-HBS	1.04	IR, 25°C, dry, CO <sub>2</sub> 415 ppm	N <sub>2</sub> purge, 105°C	-	Almost no capacity decay after 10 cycles (adsorption at 70% CO <sub>2</sub> , 75°C)	[100]
APS-MCF	1.15	Gravimetric, 25°C, dry, CO <sub>2</sub> 400 ppm	He purge, 100°C	75		[85]
MAPS-MCF	0.18	Gravimetric, 25°C, dry, CO <sub>2</sub> 400 ppm	He purge, 100°C	80	-	[85]

Adsorbent	Adsorption Capacity / mmol·g <sup>-1</sup>	Adsorption Conditions	Desorption Conditions	Adsorption Heat / kJ·mol <sup>-1</sup>	Stability	Reference
TRI-Silica gel	0.773	IR, 25°C, dry, CO <sub>2</sub> 415 ppm	N <sub>2</sub> purge, 90°C	-	Almost no capacity decay after 17 cycles	[125]
APS-Silica gel	0.30	IR, 25°C, dry, CO <sub>2</sub> 400 ppm	Vacuum, 90°C	90	Almost no capacity decay after 40 cycles	[101]
APS-Aerogel	0.72	IR, 20°C, humid, CO <sub>2</sub> 2500 ppm, RH 30%	N <sub>2</sub> purge, 70°C	—	Almost no capacity decay after 6 cycles	[126]
TRI-Aerogel	0.73	IR, 20°C, humid, CO <sub>2</sub> 2500 ppm, RH 30%	N <sub>2</sub> purge, 70°C	-	Almost no capacity decay after 8 cycles	[126]
NFC	1.39	IR, 25°C, humid, CO <sub>2</sub> 500 ppm, RH 40%	Vacuum, 90°C	-	Almost no capacity decay after 20 cycles	[89]
Lewatit 1065	1.46	IR, 25°C, humid, CO <sub>2</sub> 400 ppm, RH 70%	N <sub>2</sub> purge, 130°C	-	Almost no capacity decay after 12 cycles	[127]
Lewatit 1065	0.90	Volumetric, 25°C, dry, CO <sub>2</sub> 400 ppm	N <sub>2</sub> purge, 95°C	71	2.2% capacity decay after 30 cycles	[20]
DETA-PPN	1.04	Volumetric, 25°C, dry, CO <sub>2</sub> 400 ppm	Vacuum, 120°C	55		[91]
TRI-Mg <sub>0.5</sub> Al-O	1.05	Volumetric, 25°C, dry, CO <sub>2</sub> 400 ppm	N <sub>2</sub> purge, 80°C	70	Almost no capacity decay after 50 cycles	[83]

## 4 In-situ Polymerized Supported Amines

In in-situ polymerized supported amines, nitrogen-containing small molecule monomers undergo in-situ polymerization, forming polymeric amine structures fixed within the pores of porous supports. The synthesis process of this type of adsorbent is similar to that of grafted supported amines, but the amine and support are usually connected by C-O bonds. In grafted supported amines, only one amine molecule is attached to two hydroxyl sites of the support, and this amine typically contains only 1-5 amino groups. In in-situ polymerized supported amines, polymerization forms long polymer chains containing tens or hundreds of amino groups, thus enabling higher CO<sub>2</sub> adsorption capacity. Concurrently, the covalent attachment between amine functionalities and the support matrix imparts exceptional stability throughout repeated adsorption-desorption cycles.

### 4.1 Effect of Raw Material Ratio and Addition Method

Simultaneously, the covalent attachment between amine functionalities and the support matrix imparts exceptional stability throughout repeated adsorption-desorption cycles. In-situ polymerized supported amines were initially developed by Rosenholm and colleagues in 2006, who separately prepared aziridine and SBA-15 before conducting a single-step polymerization employing toluene as solvent and acetic acid as catalyst. This transformation proceeded under reflux at 75°C within an inert argon environment. The resulting product was subsequently purified through toluene washing, filtration, and vacuum drying at 40°C to yield the desired material. In 2009, Drese and co-workers investigated how reactant stoichiometry influences synthesis outcomes, establishing that the aziridine-to-SBA-15 proportion strongly correlates with both amine content and ultimate CO<sub>2</sub> capture performance. Their findings identified an optimal aziridine/SBA-15 ratio of 2.65, enabling amine loadings of 9.78 mmol/g. Under these optimized conditions, the material achieved 5.55 mmol/g CO<sub>2</sub> uptake at 25°C and 104 Pa partial pressure under humid conditions. Drese et al. also found that the raw material addition method significantly affected the amine loading effect. They compared adding aziridine dropwise over 90 minutes with adding it all at once at the beginning of the reaction. The findings indicated that gradual dropwise introduction resulted in diminished amine incorporation compared to single-batch addition. The findings indicated that gradual dropwise introduction resulted in diminished amine incorporation compared to single-batch addition, yielding loadings of 4.46 mmol/g versus 7.37 mmol/g, respectively. This disparity presumably stems from variations in aziridine concentration gradients existing between the support's internal voids and the surrounding bulk medium, alongside the subsequent propagation pathway of the polymerization process.

### 4.2 Effect of Nitrogen-Containing Monomers

Besides the most common use of aziridine as the nitrogen-containing small molecule, other polymerization raw materials have also been adopted. Chaikittisilp et al. used a vapor transport synthesis method, transporting azetidines or aziridine in vapor form onto/into the support, and forming polypropyleneimine or polyethyleneimine attached to the support via in-situ polymerization. Materials synthesized from azetidine through this methodology demonstrated superior thermal robustness compared to aziridine-based equivalents, as revealed by differential thermogravimetric profiles. Additionally, when fabricated under equivalent conditions (reaction time, temperature, support type, and cyclic monomer-to-support ratio), azetidine-derived adsorbents exhibited lower organic loadings than their aziridine counterparts. This reduction in amine density presumably arises from azetidine's elevated volatility relative to aziridine. However, research exploring azetidine-based materials for CO<sub>2</sub> sequestration has yet to be documented. Chaikitatsilp et al. initially grafted 3-aminopropyltrimethoxysilane (APTMS) onto SBA-15, then coupled Z-protected L-lysine via ring-opening polymerization. Subsequent deprotection and neutralization with aqueous NaOH yielded the final product, as depicted in Fig. 10(a). This sorbent achieved amine loadings between 2.76 and 5.18 mmol/g, with a CO<sub>2</sub> uptake of 0.6 mmol/g under DAC conditions.

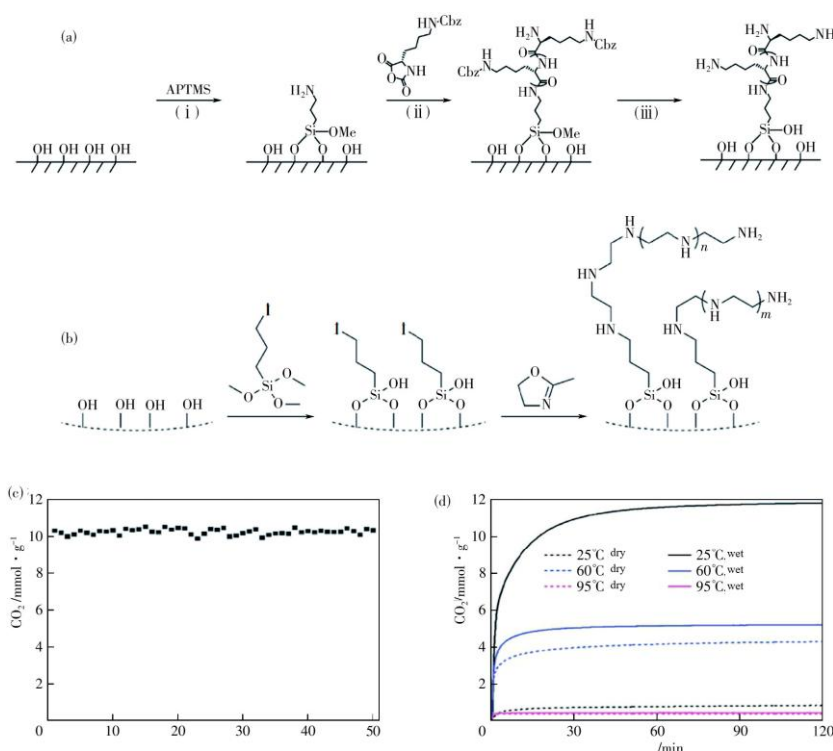


**Figure 10** The influence of nitrogen-containing monomers

Qi et al. synthesized a new in-situ polymerized supported amine using a method similar to Chaikittisilp et al. They first fixed 3-iodopropyltrimethoxysilane (IPTMS) on mesoporous silica foam as an initiator. Then, cationic polymerization of 2-methyl-2-oxazoline was performed, followed by subsequent acid hydrolysis, yielding linear polyethyleneimine polymer attached to the support. This polymer has terminal primary and secondary amines [Fig. 10(b)]. At this juncture, the sorbent displayed an overall nitrogen concentration of 15.1 mmol/g, attaining a capture capacity of 0.82 mmol/g at 25°C under anhydrous 8 vol% CO<sub>2</sub> conditions. Notably, upon introduction of 18% relative humidity, the capacity experienced a dramatic enhancement to 11.8 mmol/g. The material furthermore exhibited exceptional cycling durability, showing merely 1% degradation across 30 consecutive adsorption-regeneration cycles, as depicted in Fig. 10(c). Packed-column evaluation employing synthetic flue gas (25°C, 8 vol% CO<sub>2</sub>, 18% RH) demonstrated swift CO<sub>2</sub> sequestration, achieving 9 mmol/g within the initial hour. Following five hours, the uptake equilibrated at roughly 12 mmol/g, corroborating thermogravimetric data [Fig. 10(d)]. The sorbent also manifested rapid release characteristics under flow conditions, undergoing complete thermal regeneration at 100°C within a half-hour timeframe.

### 4.3 Effect of Porous Supports

Porous supports play a key role in the synthesis of supported amines and their CO<sub>2</sub> capture performance. Their pore size, pore volume, and surface properties significantly affect amine loading, polymer structure, and adsorption performance.

The dimensions and void space of support pores exert direct control over reactant transport, the extent of polymer branching, and final amine content. According to Drese and co-authors, aziridine undergoes cationic ring-opening polymerization (CROP) as a swift, difficult-to-regulate process. Restrictive pore apertures within supports may impede reactant movement, consequently altering both the branching frequency and chain length of the generated polymer, potentially culminating in pore occlusion. Illustratively, Mahinpey and colleagues reported that pore-enlarged SBA-15 delivered merely 0.27 mmol/g CO<sub>2</sub> uptake at 400 ppm concentration, whereas this value climbed to 0.94 mmol/g when exposed to 15% CO<sub>2</sub>, demonstrating the advantageous role of expanded pores in enhancing sorption efficiency.

Surface attributes of supports—encompassing hydroxyl population, acid-base character, and wetting behavior—profoundly impact amine fixation and CO<sub>2</sub> capture effectiveness. Specifically, silanol groups native to silica exhibit mild Brønsted acidic properties adequate for promoting aziridine ring-opening throughout CROP, obviating the requirement for external acetic acid catalysis. By comparison, cellulose-derived aerogels display diminished surface hydroxyl availability coupled with fibrous morphologies that constrain amine incorporation (1.56 mmol/g), yielding substantially inferior CO<sub>2</sub> sequestration relative to silica-based aerogels. Kong et al. synthesized various amine-containing hybrid aerogels through a unified sol-gel protocol, subsequently implementing supercritical drying for trace-level CO<sub>2</sub> removal. Additionally, spherical amine hybrid aerogels were fabricated via the ball-drop approach (Fig. 11). Leveraging the substantial specific surface area and expansive interconnected mesoporous network characteristic of aerogels, these substances preserved considerable porosity despite high-density in-situ polymerization (exemplified by 7.64 mmol/g amine loading). The resultant amine-silica hybrid aerogel manifested impressive sorption capabilities, achieving 5.55 mmol/g under moisture-saturated 1% CO<sub>2</sub> flow at room temperature. Furthermore, Liu et al. fixed aziridine onto hydroxylated graphene (HG). Benefiting from the high thermal conductivity and strong binding force of graphene, the prepared supported amine showed excellent stability, decreasing by only 1% over 30 adsorption-desorption cycles.

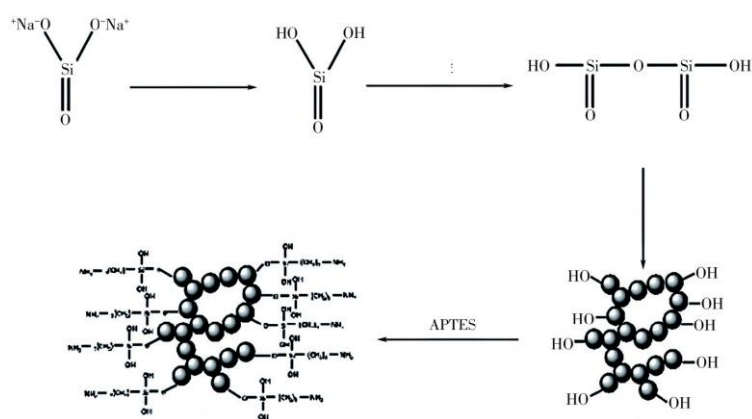


**Figure 11** Synthesis process of spherical amine functionalized silica gel

Differences in pore size, surface properties, and thermal conductivity among different supports significantly affect the performance of supported amines. Mesoporous silica foam (MSF) possesses extensive porous architectures that facilitate increased loading of amine functionalities, thereby attaining a CO<sub>2</sub> sequestration capacity of 1.50 mmol/g when exposed to 65% relative humidity at 25°C. On the other hand, the hybrid titania/siloxane aerogel system, through the integration of transition metal-based precursors, manifests a superior sorption capability of 1.64 mmol/g under 400 ppm CO<sub>2</sub> conditions. These studies indicate that the selection of supports needs to comprehensively consider factors such as pore size, surface properties, and thermal conductivity to optimize the synthesis of supported amines and their CO<sub>2</sub> capture performance.

#### 4.4 Effect of Polymerization Environment

During the polymerization process, the solvent plays multiple roles. The solvent must fulfill three critical functions: initially, it should uniformly disperse the support material throughout agitation to guarantee homogeneous solution blending and minimize mass transfer limitations for aziridine reaching the support surface; subsequently, it ought to solubilize aziridine completely within the reaction mixture; ultimately, it must remain chemically unreactive toward both aziridine and the support, thereby excluding protic solvents from consideration. Beyond these fundamental requirements, supplementary solvent attributes—such as dielectric constant and dipole moment—may additionally influence the process. Drese and colleagues investigated various solvents [including toluene, tetrahydrofuran (THF), dichloromethane (DCM), diethyl ether, and acetonitrile (ACN)] for synthetic applications. Employing glacial acetic acid as catalyst, they conducted reactions under vigorous agitation at ambient temperature within a sealed vessel. When toluene served as the reaction medium, substantial product phase separation occurred, producing a white gelatinous deposit on container walls—behavior explained by the pronounced hydrophilic nature of the amino polymer. Upon sufficient polymer accumulation on the support, particulate agglomeration ensued driven by exclusion from the surrounding organic phase. Similar aggregation was observed when using diethyl ether as the solvent, but less than with toluene. However, no such aggregation effect was observed when using dichloromethane (DCM), acetonitrile (ACN), and tetrahydrofuran (THF) as solvents. The organic loading of all other solvent samples was much lower than when using toluene. These differences can be attributed to the hydrogen bonding or polarity of different solvents, which may affect the polymerization of amines or reduce the attachment of organic compounds to the support surface. Solvents exhibiting diminished dielectric constants can establish a thermodynamic driving force that facilitates aziridine migration toward the more hydrophilic internal environments of support pores, consequently promoting enhanced diffusional transport. In cationic ring-opening polymerization (CROP), acid catalysts combined with organic solvents generally produce branched polyethyleneimine architectures. However, supercritical or vapor transport methods can eliminate the need for both solvents and acidic reagents. The vapor transport approach employs acidic silica supports to trigger nucleophilic ring-opening polymerization of aziridine solvent-free, though this demands prolonged reaction times and high-temperature environments. In contrast, supercritical carbon dioxide operates as a reaction medium that facilitates swift processing at milder temperatures. López-Aranguren and collaborators utilized compressed CO<sub>2</sub> acting dually as catalyst and solvent for in-situ aziridine polymerization inside MCM-41 and silica gel frameworks (Fig. 12). They performed comprehensive studies on variable reaction conditions: 25–45°C temperature range, 1.0–10 MPa pressure range, and 20–400 minute time intervals. This preparation method achieved substantial amine densities (6–8 mmol/g) within relatively short periods. The obtained supported amine products exhibited CO<sub>2</sub> sorption capacities of 0.95 mmol/g (MCM-41-derived) and 0.68 mmol/g (silica gel-derived) in dry 10% CO<sub>2</sub> at 25°C.

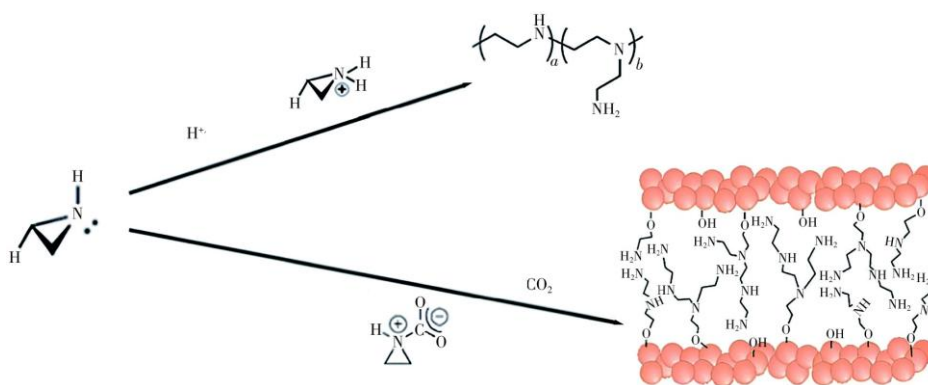


**Figure 12** Ring-opening polymerization process of azetidine under acid catalysis and CO<sub>2</sub> catalysis

In summary, changing the starting materials, reaction conditions, and amine loading can lead to structural differences in in-situ polymerized supported amines, thereby regulating their CO<sub>2</sub> adsorption capacity and kinetics. Therefore, subsequent research should deepen the understanding of the reaction mechanism during polymerization, find design paths to optimize performance, and achieve the development of more efficient in-situ polymerized supported amines. Table 3 shows the adsorption performance of in-situ polymerized supported amines reported in recent literature.

**Table 3** Adsorption Performance of In-situ Polymerized DAC Supported Amines

Adsorbent	Adsorption Capacity / mmol·g <sup>-1</sup>	Adsorption Conditions	Desorption Conditions	Adsorption Heat / kJ·mol <sup>-1</sup>	Stability	Reference
Aziridine-SBA-15	1.72	Mass spectrometry, 25°C, humid, CO <sub>2</sub> 400 ppm	Ar purge, 110°C	—	Almost no capacity decay after 4 cycles	[128]
MAHSM	1.68	TGA, 30°C, humid, CO <sub>2</sub> 400 ppm, RH 60%	He purge, 80°C	85	Almost no capacity decay after 50 cycles	[140]
PL-0.75	0.6	Gravimetric, 25°C, dry, CO <sub>2</sub> 400 ppm	Ar purge, 110°C	—	Almost no capacity decay after 3 cycles	[127]
MPS-LA-120	2.65	Gravimetric, 50°C, dry, CO <sub>2</sub> 400 ppm	Ar purge, 110°C	68	2% capacity decay after 120 cycles (adsorption at 10% CO <sub>2</sub> )	[141]
AHTSA	1.64	Gravimetric, 30°C, dry, CO <sub>2</sub> 400 ppm	N <sub>2</sub> purge, 90°C	—	Almost no capacity decay after 15 cycles	[68]
AH-RFSA	1.80	Gravimetric, 25°C, dry, CO <sub>2</sub> 450 ppm	N <sub>2</sub> purge, 80°C	—	Almost no capacity decay after 30 cycles	[142]

## 5 Conclusion

This article systematically reviews the research progress of impregnated, grafted, and in-situ polymerized supported amine DAC adsorbents. Impregnated supported amines, with their simple preparation process and relatively low cost, have advantages for large-scale production. By selecting different porous supports and organic amines, and optimizing impregnation conditions, their adsorption performance can be regulated to a certain extent. However, they face issues such as organic amine loss, uneven loading, and sensitivity to water vapor during adsorption-desorption cycles, limiting their practical application.

Grafted supported amines significantly improve the loading stability of organic amines by fixing them onto the support surface via chemical bonding. This enables the adsorbent to maintain relatively stable adsorption performance over multiple cycles. Compared to impregnated supported amines, grafted ones also show some improvement in adsorption capacity and selectivity. However, the preparation process of this method is relatively complex, requiring specific chemical reaction conditions and reagents, which increases production costs and limits its large-scale application.

In-situ polymerized supported amines utilize in-situ polymerization to directly form organic amine polymers on the support, achieving uniform distribution of organic amines. This distinctive fabrication approach imparts the adsorbent with favorable sorption characteristics, including elevated uptake capacity and rapid adsorption kinetics. However, controlling the in-situ polymerization process is difficult, requiring stringent conditions for initiators, monomers, and polymerization reaction conditions, and also has high compatibility requirements for the support. These factors hinder its further development.

Although current supported amine adsorbents have made some progress in the field of direct air capture of CO<sub>2</sub>, they still face many challenges and have some significant shortcomings, including high material cost, possible chemical degradation after multiple cycles, high energy consumption for the desorption process, and potential interference of CO<sub>2</sub> selectivity by moisture and other gases. To solve these difficulties, in-depth research and breakthroughs are needed in multiple aspects.

With respect to enhancing sorption performance, both uptake capacity and selectivity require further improvement. On one hand, designing and synthesizing novel organic amines with special structures and functions to introduce more active sites or optimize the spatial distribution of amine groups can enhance their specific binding ability with CO<sub>2</sub>. For example, developing organic amine molecules containing multiple different types of amine groups, utilizing the synergistic effect of different amine groups to improve CO<sub>2</sub> adsorption selectivity. On the other hand, further exploring new porous materials as supports.

Cost is a key factor restricting the large-scale application of supported amine adsorbents. In the future, costs need to be reduced from multiple perspectives. In terms of preparation process, optimizing existing preparation methods, simplifying operational procedures, and reducing energy consumption and raw material waste. For example, developing greener and more efficient impregnation methods to reduce solvent use and recovery costs; exploring continuous production processes for in-situ polymerization to improve production efficiency. Additionally, finding inexpensive and widely available raw materials to replace some expensive organic amines and support materials is also an important way to reduce costs.

Stability is another important issue for the practical application of supported amine adsorbents. Under realistic atmospheric conditions, diverse gas constituents (e.g., O<sub>2</sub>, N<sub>2</sub>, H<sub>2</sub>O) are present together with changing temperature and humidity, each potentially degrading adsorbent stability. Hence, techniques involving surface modification and composite structural design are crucial for improving anti-interference ability and preserving structural integrity. For example, applying hydrophobic coatings to the adsorbent surface can reduce water vapor interference with adsorption performance, while constructing multilayer composite structures can enhance the mechanical and chemical stability of the adsorbent in complex environments. With the continuous deepening of research and sustained technological innovation, supported amine adsorbents are expected to make greater breakthroughs in the field of direct air capture of CO<sub>2</sub>, making important contributions to achieving global carbon emission reduction goals.

With the continuous deepening of research and sustained technological innovation, supported amine adsorbents are expected to make greater breakthroughs in the field of direct air capture of CO<sub>2</sub>, making important contributions to achieving global carbon emission reduction goals.

## References

- [1] Feng X D, Zhang Y N, Jiang Y Q, et al. Spatiotemporal distribution and influencing factors of soil microplastic pollution: A global analysis [J]. *Environmental Science*, 2026, 47(5), doi: 10.13227/j.hjxk.202504128.
- [2] ZHENG Huidong. The source of antibiotics in aquatic environment and its impact on human health[J]. *Journal of Environmental Hygiene*, 2018, 8(1): 73-77.
- [3] LIU Qing, ZHONG Lubin, ZHAO Quanbao, et al. Synthesis of Fe<sub>3</sub>O<sub>4</sub>/polyacrylonitrile composite electrospun nanofiber mat for effective adsorption of tetracycline[J]. *ACS Applied Materials & Interfaces*, 2015, 7(27): 14573-14583.
- [4] ZENG Zhuotong, YE Shujing, WU Haipeng, et al. Research on the sustainable efficacy of g-MoS<sub>2</sub> decorated biochar nanocomposites for removing tetracycline hydrochloride from antibiotic-polluted aqueous solution[J]. *The Science of the Total Environment*, 2019, 648: 206-217.
- [5] QIAO Disi, LI Zehao, DUAN Jinyou, et al. Adsorption and photocatalytic degradation mechanism of magnetic graphene oxide/ZnO nanocomposites for tetracycline contaminants[J]. *Chemical Engineering Journal*, 2020, 400: 125952.
- [6] SUN Hongwei, YANG Jingjie, WANG Yue, et al. Study on the removal efficiency and mechanism of tetracycline in water[J]. *Coatings*, 2021, 11(11): 1354.
- [7] ZHENG Shimei, WANG Yandong, CHEN Cuihong, et al. Current progress in natural degradation and enhanced removal techniques of antibiotics in the environment: A review[J]. *International Journal of Environmental Research and Public Health*, 2022, 19(17): 10919.
- [8] ZHANG Peizhen, LI Yanfei, CAO Yaoyao, et al. Characteristics of tetracycline adsorption by cow manure biochar prepared at different pyrolysis temperatures[J]. *Bioresource Technology*, 2019, 285: 121348.
- [9] MA Yongfei, LI Ming, LI Ping, et al. Hydrothermal synthesis of magnetic sludge biochar for tetracycline and ciprofloxacin adsorptive removal[J]. *Bioresource Technology*, 2021, 319: 124199.
- [10] LIANG Huagen, ZHU Chenxi, JI Shan, et al. Magnetic Fe<sub>2</sub>O<sub>3</sub>/biochar composite prepared in a molten salt medium for antibiotic removal in water[J]. *Biochar*, 2022, 4(1): 3.
- [11] ZHANG Qingfa, CAI Hongzhen, YI Weiming, et al. Biocomposites from organic solid wastes derived biochars: A review[J]. *Materials*, 2020, 13(18): 3923.
- [12] LIANG Meina, LU Lin, HE Huijun, et al. Applications of biochar and modified biochar in heavy metal contaminated soil: A descriptive review[J]. *Sustainability*, 2021, 13(24): 14041.
- [13] DAI Xiaohu. Applications and perspectives of sludge treatment and disposal in China[J]. *Science*, 2020, 72(6):

- 30-34.
- [14] ZHOU Shanlei, XU Yabing, ZHANG Yuxi, et al. Preparation of sludge-based biochar and its adsorption to reactive black 5 dye[J]. *Shandong Chemical Industry*, 2023, 52(17): 239-241.
  - [15] HE Dandan, ZHANG Zeyu, LIU Juanli, et al. Application of municipal sludge biochar in wastewater adsorption treatment[J]. *Fine Chemicals*, 2024(7): 1447-1457.
  - [16] DEVI Parmila, SAROHA Anil K. Utilization of sludge based adsorbents for the removal of various pollutants: A review[J]. *The Science of the Total Environment*, 2017, 578: 16-33.
  - [17] FEI Yongxin, MA Huiqiang, LI Shuang. Study on adsorption performance of modified activated sludge biochar for phenol in water[J]. *Journal of Liaoning Petrochemical University*, 2022, 42(3): 19-24.
  - [18] ZHANG Xu, SHU Xin, ZHOU Xiaolin, et al. Magnetic reed biochar materials as adsorbents for aqueous copper and phenol removal[J]. *Environmental Science and Pollution Research International*, 2023, 30(2): 3659-3667.
  - [19] KASERA Nitesh, AUGOUSTIDES Victoria, KOLAR Praveen, et al. Effect of surface modification by oxygen-enriched chemicals on the surface properties of pine bark biochars[J]. *Processes*, 2022, 10(10): 2136.
  - [20] HE Xian, HONG Zhineng, JIANG Jun, et al. Enhancement of Cd(II) adsorption by rice straw biochar through oxidant and acid modifications[J]. *Environmental Science and Pollution Research International*, 2021, 28(31): 42787-42797.
  - [21] GUO Zijing, CHEN Xin, HANG Jiacheng, et al. Oxidative magnetization of biochar at relatively low pyrolysis temperature for efficient removal of different types of pollutants[J]. *Bioresource Technology*, 2023, 387: 129572.
  - [22] LIU Sen, LI Jihui, XU Shuang, et al. A modified method for enhancing adsorption capability of banana pseudostem biochar towards methylene blue at low temperature[J]. *Bioresource Technology*, 2019, 282: 48-55.
  - [23] LIN Shenglun, ZHANG Hongjie, CHEN Wei-Hsin, et al. Low-temperature biochar production from torrefaction for wastewater treatment: A review[J]. *Bioresource Technology*, 2023, 387: 129588.
  - [24] WU Jingqi, WANG Tongshuai, LIU Yuyan, et al. Norfloxacin adsorption and subsequent degradation on ball-milling tailored N-doped biochar[J]. *Chemosphere*, 2022, 303(Pt 3): 135264.
  - [25] HUANG Zhexi, YI Yunqiang, ZHANG Nuanqin, et al. Removal of fluconazole from aqueous solution by magnetic biochar treated by ball milling: Adsorption performance and mechanism[J]. *Environmental Science and Pollution Research International*, 2022, 29(22): 33335-33344.
  - [26] SHAN Danna, DENG Shubo, ZHAO Tianning, et al. Preparation of ultrafine magnetic biochar and activated carbon for pharmaceutical adsorption and subsequent degradation by ball milling[J]. *Journal of Hazardous Materials*, 2016, 305: 156-163.
  - [27] HE Juan, TANG Jingchun, ZHANG Zheng, et al. Magnetic ball-milled FeS@biochar as persulfate activator for degradation of tetracycline[J]. *Chemical Engineering Journal*, 2021, 404: 126997.
  - [28] WEI Zehua, LI Haihong, JIA Miaomiao, et al. NaOH-ball-milled co-modified magnetic biochar and its oil adsorption properties[J]. *Particuology*, 2023, 83: 40-49.
  - [29] GUO Tianxiang, ZHANG Yonghe, GENG Yuhan, et al. Surface oxidation modification of nitrogen doping biochar for enhancing CO<sub>2</sub> adsorption[J]. *Industrial Crops and Products*, 2023, 206: 117582.
  - [30] ZHANG Dawei, HE Qianqian, HU Xiaolan, et al. Enhanced adsorption for the removal of tetracycline hydrochloride(TC) using ball-milled biochar derived from crayfish shell[J]. *Colloids and Surfaces A: Physicochemical and Engineering Aspects*, 2021, 615: 126254.
  - [31] CAI Siying, ZHANG Weijun, CHEN Kang, et al. Preparation of Chinese medicine wastes biochar and its adsorption characteristics to tetracycline in water[J]. *Safety and Environmental Engineering*, 2022, 29(3): 178-186.
  - [32] MEI Yanglu, XU Jin, ZHANG Yin, et al. Effect of Fe-N modification on the properties of biochars and their adsorption behavior on tetracycline removal from aqueous solution[J]. *Bioresource Technology*, 2021, 325: 124732.
  - [33] ZHAO Zhendong, WU Qianqian, NIE Tiantian, et al. Quantitative evaluation of relationships between adsorption and partition of atrazine in biochar-amended soils with biochar characteristics[J]. *RSC Advances*, 2019, 9(8): 4162-4171.
  - [34] YANG Hucheng, YU Hao, WANG Jiahao, et al. Magnetic porous biochar as a renewable and highly effective adsorbent for the removal of tetracycline hydrochloride in water[J]. *Environmental Science and Pollution Research*, 2021, 28(43): 61513-61525.
  - [35] ZOU Chenglong, WU Qin, NIE Fahui, et al. Application of magnetic porous graphite biochar prepared

- through one-step modification in the adsorption of tetracycline and ciprofloxacin from aqueous solutions[J]. *Waste and Biomass Valorization*, 2024, 15(3): 1477-1494.
- [36] ZHANG Qingle, WANG Zhong, LI Rui. Adsorption characteristics of tetracycline on biochar from *salvia miltiorrhiza*[J]. *Shandong Chemical Industry*, 2022, 51(19): 47-50.
- [37] DHIBAR Subhendu, PAL Suchetana, KARMAKAR Kripasindhu, et al. Two novel low molecular weight gelator-driven supramolecular metallo gels efficient in antimicrobial activity applications[J]. *RSC Advances*, 2023, 13(47): 32842-32849.
- [38] OULD M'HAMED Mohamed. Ball milling for heterocyclic compounds synthesis in green chemistry: A review[J]. *Synthetic Communications*, 2015, 45(22): 2511-2528.
- [39] SHI Qiyu, WANG Wangbo, ZHANG Hongmin, et al. Porous biochar derived from walnut shell as an efficient adsorbent for tetracycline removal[J]. *Bioresource Technology*, 2023, 383: 129213.
- [40] FAN Shisuo, FAN Xinru, WANG Shuo, et al. Effect of chitosan modification on the properties of magnetic porous biochar and its adsorption performance towards tetracycline and Cu<sup>2+</sup>[J]. *Sustainable Chemistry and Pharmacy*, 2023, 33: 101057.
- [41] KIM Ji Eun, BHATIA Shashi Kant, SONG Hak Jin, et al. Adsorptive removal of tetracycline from aqueous solution by maple leaf-derived biochar[J]. *Bioresource Technology*, 2020, 306: 123092.
- [42] FAN Shisuo, TANG Jie, WANG Yi, et al. Biochar prepared from co-pyrolysis of municipal sewage sludge and tea waste for the adsorption of methylene blue from aqueous solutions: Kinetics, isotherm, thermodynamic and mechanism[J]. *Journal of Molecular Liquids*, 2016, 220: 432-441.
- [43] QI Liqiang, TENG Fei, DENG Xin, et al. Experimental study on adsorption of Hg(II) with microwave-assisted alkali-modified fly ash[J]. *Powder Technology*, 2019, 351: 153-158.
- [44] ZHANG Juanxiang, ZHAO Baowei, MA Fengfeng, et al. Adsorption characteristics and mechanism of tetracycline by biochars derived from paper industry sludge[J]. *China Environmental Science*, 2020, 40(9): 3821-3828.
- [45] HUANG Hui, GUAN Yingbing, SUN Xuwei, et al. Adsorption behavior of chlortetracycline on the biochar-based magnetic gel balloon[J]. *Technology of Water Treatment*, 2023, 49(7): 32-37.
- [46] LIU Juanli, ZHOU Baiqin, ZHANG Hong, et al. A novel biochar modified by chitosan-Fe/S for tetracycline adsorption and studies on site energy distribution[J]. *Bioresource Technology*, 2019, 294: 122152.
- [47] MA Juan, ZHOU Baiqin, ZHANG Hong, et al. Fe/S modified sludge-based biochar for tetracycline removal from water[J]. *Powder Technology*, 2020, 364: 889-900.
- [48] FAN Fangfang, TONG Zhongkai, ZUO Weiyuan. Study on adsorption of tetracycline from wastewater by calcium modified peanut shell biochar[J]. *Inorganic Chemicals Industry*, 2023, 55(6): 109-115.
- [49] LIN Bingfeng, CHEN Zhihao, YANG Fangli, et al. Adsorption performance of tetracycline by manganese ferrite-modified biochar[J]. *Journal of Agro-Environment Science*, 2023, 42(7): 1585-1596.
- [50] XU Jin, MA Yifan, YAO Guoqing, et al. Effect of KOH activation on the properties of biochar and its adsorption behavior on tetracycline removal from an aqueous solution[J]. *Environmental Science*, 2022, 43(12): 5635-5646.
- [51] ZHAO Zhiwei, CHEN Chen, LIANG Zhijie, et al. Enhanced adsorption activity of manganese oxide-modified biochar for the removal of tetracycline from aqueous solution[J]. *Journal of Agro-Environment Science*, 2021, 40(1): 194-201.
- [52] LI Guoting, LI Kangli, ZHANG Shuaiyang, et al. Comparative study on adsorption of methylene blue and tetracycline by lignocellulosic biochar[J]. *Jiangsu Agricultural Sciences*, 2021, 49(18): 234-240.
- [53] LI Bin, ZHANG Yin, XU Jin, et al. Effect of carbonization methods on the properties of tea waste biochars and their application in tetracycline removal from aqueous solutions[J]. *Chemosphere*, 2021, 267: 129283.
- [54] QU Jianhua, ZHANG Bo, TONG Hua, et al. High-efficiency decontamination of Pb(II) and tetracycline in contaminated water using ball-milled magnetic bone derived biochar[J]. *Journal of Cleaner Production*, 2023, 385: 135683.
- [55] WANG Kaifeng, YAO Runlin, ZHANG Dongqing, et al. Tetracycline adsorption performance and mechanism using calcium hydroxide-modified biochars[J]. *Toxics*, 2023, 11(10): 841.
- [56] LIU Sen. Study on modification of banana pseudostem biochar and its adsorption properties for methylene blue[D]. Haikou: Hainan University, 2020.